

Forsmark site investigation

**Boreholes KFM01D, KFM08C, KFM09B
Characterisation of pore water**

**Part 1 Diffusion experiments and
pore-water data**

H N Waber, Rock Water Interaction, University of Bern

J A T Smellie, Conterra AB

September 2007

Svensk Kärnbränslehantering AB

Swedish Nuclear Fuel
and Waste Management Co
Box 250, SE-101 24 Stockholm
Tel +46 8 459 84 00



Forsmark site investigation

Boreholes KFM01D, KFM08C, KFM09B Characterisation of pore water

Part 1 Diffusion experiments and pore-water data

H N Waber, Rock Water Interaction, University of Bern

J A T Smellie, Conterra AB

September 2007

Keywords: Site investigations, Matrix pore water, Leaching, Diffusion, Chemistry, AP PF 400-05-116, AP PF 400-05-117.

This report concerns a study which was conducted for SKB. The conclusions and viewpoints presented in the report are those of the authors and do not necessarily coincide with those of the client.

Data in SKB's database can be changed for different reasons. Minor changes in SKB's database will not necessarily result in a revised report. Data revisions may also be presented as supplements, available at www.skb.se.

A pdf version of this document can be downloaded from www.skb.se.

Abstract

Drillcore material has been successfully sampled from boreholes KFM01D, KFM08C, and KFM09B for studies relating to characterisation of the composition of pore water that resides in the connected pore space. Accessible, interconnected pore water has been extracted successfully by laboratory out-diffusion methods using some 14, 10, and 8 samples, respectively, for the three boreholes. The methodology to extract and analyse the pore water is outlined and the analytical data are tabulated. The data are critically reviewed for their significance with respect to in situ conditions.

In boreholes KFM01D and KFM08C the connected pore space measured by two different, largely independent methods on the rock matrix samples, depends on the rock's texture and alteration state. In the unaltered rock matrix the connected porosity is low (< 0.3 vol.%) and tends to decrease with increasing depth. Changes in the chemical and isotopic composition of the pore water coincide with changes in the hydrological regime, i.e. the fracture frequency and proximity to water-conducting fractures, which in turn can reflect different structural domains. With increasing depth there occurs a change from moderately mineralised and brackish pore water of a general Na-Ca-Cl chemical type with Cl concentrations between 2 g/kgH₂O and 4 g/kgH₂O, to saline pore water of a general Ca-Na-Cl type and with Cl concentrations between 6 g/kgH₂O and 15 g/kgH₂O. In combination with the isotopic composition the pore water chemistry reflects unique compositions that cannot be associated with a single known end member or reference water or a simple mixture of these. This is consistent with the expected long residence time and long-term interaction of the pore water with fracture groundwaters that change in composition over shorter time periods.

In borehole KFM09B a pore-water profile extending from a porous, fracture episyenite zone into the unaltered rock matrix has been sampled at a depth of 470 m below surface. The Cl concentration profile suggests that the duration of saline water (> 10 g/kgH₂O) circulation in the episyenite is limited and that this was preceded by a much longer period of dilute water (meteoric \pm glacial) circulation in the episyenite.

Summary

Pore water that resides in the pore space between minerals and along grain boundaries in crystalline rocks of low permeability cannot be sampled by conventional groundwater sampling techniques and therefore has to be characterised by applying indirect methods based on drillcore material. Accessible, interconnected pore water has been extracted successfully by laboratory out-diffusion methods using some 14, 10 and 8 drillcore samples from boreholes KFM01D, KFM08C, and KFM09B, respectively, as part of the Forsmark hydrogeochemical site investigation programme. The objective was to characterise these pore waters chemically and isotopically and relate these data to the present and past groundwater evolution of the site. This report outlines the methodology to extract and analyse the pore water, tabulates the analytical data and compares the pore-water chloride and water isotope compositions: a) to the hydrologic data, such as frequency and hydraulic conductivity of nearby water-conducting fractures, and b) to the palaeohydrochemical evolution of the Forsmark area.

The pore-water investigations performed on core samples from boreholes KFM01D, KFM08C and KFM09B clearly demonstrate that the great logistic effort to sample drillcore material in its original saturated state was well worthwhile. Water contents obtained for the rock samples by two different, largely independent methods, are in close agreement indicating that the core material was neither substantially influenced by de-saturation nor by the possibility of drilling fluid penetration induced by immediate stress release in the borehole during drilling. The water content and the water-loss porosity derived from the rock samples for boreholes KFM01D and KFM08C show similar values in the first 500 m along the borehole (i.e. approx. the first 430 m below surface) and then display a decreasing trend with increasing depth to 940 m along the borehole (i.e. about 814 m below surface). This is what would be expected based on the increase in lithostatic pressure and also the local stress field. The porosity data derived by the two methods in this study contrast with porosity data derived by re-saturation techniques and clearly demonstrate that re-saturation techniques are not able to reproduce porosity data that are reliable and representative for in situ conditions when applied to crystalline rocks samples from a borehole.

In boreholes KFM01D and KFM08C the Cl concentrations of the pore water show a distinct trend with depth that is correlated with the frequency of water-conducting fractures. The Cl concentrations are around 2 g/kgH₂O in the first 200 m from where they increase continuously to 4 and 6 g/kgH₂O, respectively, down to about 550 m along the borehole. Between about 600–650 m borehole length the Cl concentrations decrease again but there is no apparent correlation to the occurrence of highly transmissive fractures. Further downwards the concentrations then increase to their highest values of 10–15 g/kgH₂O. The inferred chemical type of the pore water is of Na-Ca-Cl type down to about 650 m borehole length with the possibility of being a Na-Ca-Cl-HCO₃ type in the first 200 m. At greater depth below 650 m borehole length the pore water is of a Ca-Na-Cl type.

In borehole KFM09B studies were confined to a specific profile extending from the contact of the porous and fractured episyenite zone (573 m borehole length) into the unaltered rock matrix. Along this profile there is a distinct pattern of Cl concentrations in the pore water; i.e. the high salinity in the sample adjacent to the fracture (10.5 g/kgH₂O) drops to brackish values (4.8 g/kgH₂O) within one metre distance before it increases to “background” values (8.6 g/kgH₂O) at 13 metres distance from the episyenite. The profile suggests that the circulation of saline water in the episyenite did not yet occur over very long periods and that prior to this saline water a dilute to brackish water must have circulated in the episyenite for a considerable period of time to dilute these “background” concentrations present at 13 metres from the episyenite.

The observations made on the pore water of core material from boreholes KFM01D, KFM08C, and KFM09B suggest that dilute water must have circulated over extended periods of time in at least some fracture systems down to depths of at least 500 m vertical depth below surface. They suggest further that the circulation of dilute water was followed by that of saline water in more recent times. The origin of this saline water is not yet known because the pore water data cannot be explained by a simple combination of either of the known end member and reference water types.

Sammanfattning

Det grundvatten som förekommer i porer mellan mineral och längs korngränser i kristallint berg med låg genomtränglighet kan inte undersökas med konventionella provtagningsmetoder för grundvatten och måste därför karakteriseras genom indirekta metoder baserade på prov från borrhämlor. Tillgängligt vatten i sammanbundna porer har extraherats med framgång med hjälp av ut-diffusionsmetoder utförda i laboratorium från 14, 10 respektive 8 prov på borrhämlor från borrhämlorna KFM01D, KFM08C och KFM09B. Detta ingår som en del av det hydrogeokemiska undersökningsprogrammet inom platsundersökningarna i Forsmark. Målet var att karakterisera dessa porvatten med avseende på kemi och isotopsammansättning samt relatera erhållna data till grundvattnets utveckling på platsen både i nutid och historiskt sett. Denna rapport beskriver metodologin för att extrahera och analysera porvattnet samt ger en sammanställning av analysdata. Vidare jämförs kloridhalten och isotopsammansättningen i porvattnet med a) hydrogeologidata i form av frekvens av näraliggande vattenförande sprickor samt deras hydrauliska konduktivitet, och b) den palaeohydrokemiska utvecklingen av Forsmarksområdet.

Porvattenundersökningarna i prov på kärna från borrhämlorna KFM01D, KFM08C och KFM09B demonstrerar tydligt att de stora logistiska ansträngningar som gjorts för att ta prov på borrhämlorna i dess naturliga vattenmättade tillstånd var väl värt mödan. Vatteninnehållet i bergproven erhöles från två helt oberoende metoder och visar en nära överensstämmelse. Detta indikerar att resultaten varken var påtagligt påverkade av undermättnad eller av möjlig spolvatteninträning orsakad av den ögonblickliga tryckavlastningen som sker i borrhämlorna i samband med att den friborras. Vatteninnehållet och vatten-förlustporositeten som härrör från kärnprov för borrhämlorna KFM01D och KFM08C visar liknande värden för de första 500 m längs borrhämlorna (t ex ner till 430 m under markytan) och visar därefter en avtagande trend med ökande djup till 940 m borrhämlorlängd (t ex ca 814 m under markytan). Detta är vad som kan förväntas baserat på ökningen av det litostatiska trycket och det lokala spänningsfältet. Porositetsdata från de två metoderna i denna studie avviker från porositetsdata erhållna med tekniker som bygger på återmättnad och visar klart att de senare metoderna inte kan producera porositetsdata som är representativa för in situ förhållanden, när de tillämpas på uttagna prov från kristallint berg i borrhämlor.

I borrhämlorna KFM01D och KFM08C visar kloridkoncentrationerna i porvattnet en tydlig trend mot djupet som är korrelerad till frekvensen av vattenförande sprickor. Kloridkoncentrationerna ligger runt 2 g/kgH₂O ner till 200 m borrhämlorlängd där de ökar kontinuerligt till 4 respektive 6 g/kgH₂O vid 550 m borrhämlorlängd. Mellan 600–650 m borrhämlorlängd minskar kloridkoncentrationen igen men det finns ingen tydlig korrelation till förekomst av särskilt transmissiva sprickor. Ytterligare längre ner ökar koncentrationerna till de högsta uppmätta värdena på 10–15 g/kgH₂O. Porvattnet har tolkats som Na-Ca-Cl typ ner till 650 m borrhämlorlängd men är möjligen av Na-Ca-Cl-HCO₃ typ ner till 200 m. Vid större djup under 650 m borrhämlorlängd är porvattnet av Ca-Na-Cl typ.

Studierna i KFM09B begränsade sig till en specifik profil som sträcker sig från kontakten med den porösa och uppspruckna episyenitonen (573 m borrhämlorlängd) och in i den icke omvandlade bergmatrisen. Längs denna profil uppvisar kloridkoncentrationerna i porvattnet ett tydligt mönster, dvs den höga saliniteten i provet nära sprickan minskar till värden motsvarande bräckt vatten (4,8 g/kgH₂O) inom en meters avstånd innan den ökar till bakgrundsvärden (8,6 g/kgH₂O) vid ett avstånd på 13 meter från episyeniten. Profilen indikerar att saltvattnet i episyenitonen ännu inte har befunnits i omlopp under någon längre period och att innan dess måste ett sött till bräckt vatten ha funnits i omlopp i episyeniten under en betydande tidsperiod för att späda ut de ”bakgrundskoncentrationer” som uppmätts på 13 meters avstånd från episyeniten.

Porvattenobservationerna i material från borrhälen KFM01D, KFM08C, och KFM09B tyder på att sött/bräckt vatten måste ha funnits i omlopp under långa tidsperioder i varje fall i några spricksystem ner till ett vertikalt djup på åtminstone 500 m under markytan. De tyder vidare på att detta vatten åtföljdes av saltvatten under mer näraliggande tid. Ursprunget för detta salina vatten är inte känt ännu eftersom porvattendata inte kan förklaras genom en enkel kombination av några av de kända typvattnen och referensvattnen.

Contents

1	Introduction	11
2	Materials and methods	13
2.1	Samples and sample preparation	13
2.2	Analytical methods	14
2.3	Data handling	17
2.4	Nonconformities	17
3	KFM01D borehole: Pore-water data	19
3.1	Water content and water-loss porosity	21
3.2	Out-diffusion experiments	23
3.2.1	Equilibrium control in the out-diffusion experiment	23
3.2.2	Chemical composition of experiment solution	24
3.2.3	Implications for pore-water composition	28
3.3	Chloride composition of pore-water	28
3.4	Water-isotope composition of pore-water	30
4	KFM08C borehole: Pore-water data	33
4.1	Water content and water-loss porosity	35
4.2	Out-diffusion experiments	37
4.2.1	Equilibrium control in out-diffusion experiment	37
4.2.2	Chemical composition of experiment solutions	37
4.2.3	Implications for pore-water composition	39
4.3	Chloride composition of pore-water	42
4.4	Water-isotope composition of pore-water	43
5	KFM09B borehole: Pore-water data	47
5.1	Water content and porosity	48
5.2	Out-diffusion experiments	50
5.2.1	Equilibrium control in out-diffusion experiment	50
5.2.2	Chemical composition of experiment solutions	51
5.2.3	Implications for pore-water composition	52
5.3	Chloride composition of pore-water	54
5.4	Water-isotope composition of pore-water	55
6	Discussion	57
7	Acknowledgements	59
	References	60

1 Introduction

This document reports performance and results of the activity *characterisation of pore water* in drillcore samples within the site investigation programme at Forsmark. The drillcore samples were selected during drilling of the telescopic boreholes KFM01D, KFM08C and KFM09B in accordance with the Activity Plans AP PF 400-05-116 and AP PF 400-05-117, respectively. The location within the Forsmark site investigation area of the three boreholes considered for pore-water characterisation is given in Figure 1-1. Borehole KFM01D was drilled in the western part of the candidate area at Forsmark to provide information about the hydrogeology and hydrochemistry of a potential repository rock volume. Hydraulic flow logging indicated two major brittle deformation zones and some minor fractures, both types sufficiently transmissive to be hydrochemically sampled in the central part of the candidate area. Borehole KFM08C was drilled in the northeastern part of the candidate site, close to the western shore of Asphällsfjärden to provide hydrogeological and hydrochemical information from expected repository depths close to the boundary of the site investigation area. Borehole KFM09B was drilled south of the Forsmark nuclear power plant to provide hydrogeological information for the design of a possible access tunnel. In this borehole samples for pore-water characterisation were restricted to a profile of 13 metres extending from a highly altered, vuggy zone into the non-fractured bedrock. This vuggy episyenite formed as a result of hydrothermal quartz dissolution in the former metagranite-granodiorite and pegmatitic granite in the interval 569–573 m /Carlsten et al. 2006/. Samples for pore water studies were collected across this interval to provide additional information as to the nature of this vuggy zone, earlier subjected to a detailed mineralogical and geochemical study.

Crystalline rocks are characterised in general by two hydraulic regimes. The first regime includes the water-conducting zones related to regional or local fracture networks. The second regime includes the bedrock mass of low permeability between the water-conducting zones. Depending on the residence time of formation groundwater in the water-conducting zones, interaction with water present in the pore space of the low permeable bedrock might become significant. In addition, since repository construction will be restricted largely to bedrock of low permeability, this pore water over time will interact with the repository barrier materials (e.g. bentonite; canister) potentially leading to a deterioration in their physical properties. For safety assessment considerations it is therefore important to know the composition of such pore water and its evolution over recent geological time, certainly during the last thousands to hundreds of thousands of years in accordance with the expected lifespan of a repository. Pore-water compositions can be assessed by combining the information gained from pore-water profiles within bedrock of low permeability and the chemical and isotopic data of formation groundwaters circulating in the adjacent fracture zones.

Pore water that resides in the pore space between minerals and along grain boundaries in crystalline rocks of low permeability cannot be sampled by conventional groundwater sampling techniques and therefore has to be characterised by applying indirect methods based on drillcore material. In the recent past such techniques were successfully applied to borehole KFM06A at Forsmark /Waber and Smellie 2005/ and to borehole KLX03 at Laxemar to trace the pore water chemistry in low permeable bedrock to depths of around 1,000 m /Waber and Smellie 2006/.

A similar approach has been carried out for boreholes KFM01D; KFM08C and KFM09B. Based on the knowledge obtained from studies performed on borehole KFM06A, detailed mineralogical and fluid inclusion studies otherwise necessary for pore water characterisation, have not been carried out for these boreholes and the investigations have been restricted to different diffusion methods and measurements of petrophysical properties. This report presents the methodologies employed, a compilation of the resulting analytical data from the various experiments, and the derived pore-water data.

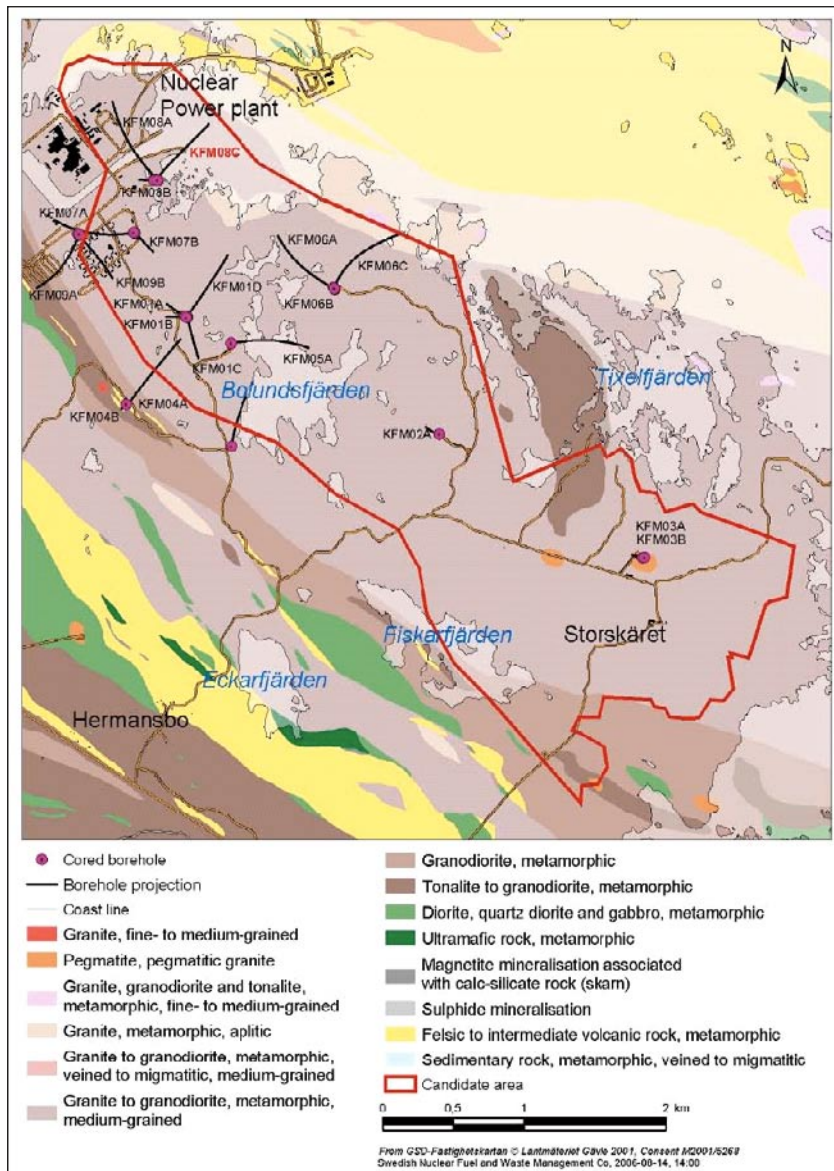


Figure 1-1. Generalised geological map of the Forsmark site investigation area and the projection of boreholes KFM01D, KFM08C and KFM09B used for pore-water characterisation.

2 Materials and methods

Drillcore sections of about 25–45 cm in length were taken at regular depth intervals of approximately 50 m from boreholes KFM01D and KFM08C. The sampling protocol required the samples to be taken from homogeneous, non-fractured bedrock volumes at least 5 metres away from any water-conducting fractures or fracture zones. To safeguard against the selection of unsuitable samples, which might not be obvious at the time, extra core lengths were taken along the borehole length when good rock properties occurred. From borehole KFM09B drillcore sections were taken adjacent to the highly altered and porous zone below 573.45 metres on a dm to m scale.

An important requirement for pore water characterisation using rock samples is the preservation of the fully water-saturated state of the rock material immediately following drilling and sampling and during transportation from the site to the laboratory. This precaution is to inhibit possible water-rock interactions induced by exposure of the rock sample to air. To minimise these potential perturbing effects the samples were immediately wiped clean with a damp towel following drilling and selection, wrapped into a heavy-duty PVC bag which was repeatedly flushed with nitrogen, evacuated and heat sealed. This procedure was repeated with a second PVC bag and finally sealed in a plastic coated Al-foil. The samples were then air freighted to the laboratory at the University of Bern, Switzerland, where they were immediately stored at 4°C in a cooling room and prepared for the various measurements and experiments within about 20 hours after arrival.

Once exposed to the air and/or stored over too long a time period, the drillcore samples lose their value for pore water characterisation. Therefore, all samples received had to be rapidly conditioned so that the different laboratory experimental procedures could be initiated. For the out-diffusion experiments this involved all samples collected for pore water characterisation, i.e. 14 drillcore samples from borehole KFM01D, 10 drillcore samples from borehole KFM08C, and 8 drillcore samples from borehole KFM09B.

Based on a personal on-site drillcore inspection, and the use of available drillcore mapping information, BIPS logs and also hydraulic data from downhole differential flow measurements, it was decided to analyse for all samples the chemical composition of the out-diffusion experiment solutions and the water isotope composition of the isotope diffusive-exchange experiments. A final decision to analyse the isotopic composition of strontium and chloride in the out-diffusion experiment solutions has still to be made.

2.1 Samples and sample preparation

For legibility reasons the sample labelling adopted in this report is a subsequent numbering of the samples with depth using the borehole name as prefix; similar labelling was used for the laboratory studies. For each borehole, the conversion of this sample description to the SKB sample number and the length along borehole is given in the first table of the following chapters (Table 3-1). The analytical programme performed on the rock samples and experiment solutions is given for each borehole in the second table of the following chapters (Table 3-2).

Following arrival at the laboratory the core sections were cut by dry sawing into full-diameter samples of about 19 cm length to be used specifically for the out-diffusion experiments. In several cases the length of drillcore obtained was too short and this required an adjustment of the experimental set-up to accommodate core pieces of 12 cm length instead. The only observed drawback of this shorter sample length is the smaller volume of experiment solution obtained that does not allow all planned isotope analyses to be carried out. The remaining material from

the top and bottom of the core section was used for the diffusive isotope equilibration method and the determination of the water content. The wet weight of such material was determined immediately after unpacking and preparation.

2.2 Analytical methods

Most of the analytical work of this study has been conducted at the Institute of Geological Sciences, University of Bern, Switzerland. Thus, if not otherwise stated the analytics have been performed at this institution.

The water content was determined by the gravimetric determination of the water loss by drying subsamples at 105°C until stable weight conditions (± 0.002 g). If the material received allowed it, then the weight of these samples was chosen to be more than about 200 g to minimise possible de-saturation effects and to account for variations in the grain size of the rocks. For the same reasons, intact drillcore pieces were used without creating unnecessary new surfaces by cutting and/or breaking. It is important to note that drying to stable-weight conditions of such large-sized samples might take several weeks.

The water content, WC, was also determined on the material used for the diffusive isotope equilibration method using the same technique. These samples remained saturated throughout the experiment because they were placed in a vapour-tight vessel at 100% humidity during the equilibration procedure (see also below). The water-loss porosity was calculated from the water loss and the volumetrically determined bulk wet density.

A measure for the bulk wet density, $\rho_{\text{bulk, wet}}$, of the rocks investigated was obtained from the volume and saturated mass of the core samples used for out-diffusion experiments. The volume was calculated from measurements of height and diameter of the core samples using a vernier calliper with an error of ± 0.01 mm. Variations in the core diameter over the lengths of the samples was found to be less than 0.05 mm for most samples and a constant diameter was used in the calculation of the volume. For the so-derived wet bulk density this results in an error of less than 3%.

The water-loss porosity, Φ_{WL} , was then approximated using the water content and the bulk wet density according to:

$$\Phi_{\text{WL}} = WC_{\text{wet}} \cdot \frac{\rho_{\text{bulk, wet}}}{\rho_{\text{water}}} \quad (1)$$

The stable isotope composition of the pore water was determined by the isotope diffusive isotope equilibration technique (see /Waber and Smellie 2005, 2006/ for details and references). In this method the isotope exchange occurs through the gaseous phase without any direct contact between the rock sample and the test water. Rock pieces of about 1 cm in diameter from the centre of the core and a small petri dish filled with a test water are stored together in a vapour-tight glass container. The mass and stable water isotope composition of the test water are known. In the test water about 0.3 mol NaCl are dissolved to lower the water vapour pressure above the test-water surface. This is to minimise loss of test water from the petri dish and condensation on the rock fragments and the glass container walls. The petri dish with the test water and the whole container are weighed before and after the exchange experiment to check that no water is lost from the container and there was no transfer of test water to the sample by possible sorption on the rock material. Isotopic equilibrium in this system is achieved in about 20 to 30 days at room temperature depending on the size and water content of the rock pieces. After complete equilibration the two test waters were removed and analysed by conventional ion-ratio mass spectrometry at Hydroisotop GmbH, Germany. The results are reported relative to the V-SMOW standard with a precision of $\pm 0.15\%$ for $\delta^{18}\text{O}$ and $\pm 1.5\%$ for $\delta^2\text{H}$.

The diffusive isotope equilibration method was originally designed for rocks with water contents in the order of several percent. To account for the much lower water content in the crystalline rocks from the Forsmark area, the method was modified in that an artificial test water was used, which is strongly enriched in ^2H and depleted in ^{18}O ($\delta^{18}\text{O} = -109.27\text{‰}$ and $\delta^2\text{H} = +424.1\text{‰}$ V-SMOW). In addition, smaller volumes of test water and larger masses of rock were used. These modifications were necessary in order to obtain a modified test water composition after equilibration that is outside the standard analytical error of the mass-spectrometer. Obviously, solutions so much enriched in ^2H are difficult to analyse for $\delta^2\text{H}$ and certain memory effects cannot be excluded for some of the samples. In contrast, the oxygen isotope data are more reliable.

If successful, the diffusive isotope equilibration method delivers the stable isotope composition of pore water and the mass of pore water present in the connected pore space of the rock sample. The mass of pore water can be derived from the relation:

$$M_{PW} = \frac{M_{TW1} \cdot (C_{TW1}^{\infty} - C_{TW1}^0) + M_{TW2} \cdot (C_{TW2}^0 - C_{TW2}^{\infty})}{C_{TW2}^{\infty} - C_{TW1}^{\infty}} \quad (2)$$

where M = mass, C 1,2 = concentration of isotope tracer 1 and 2 in the test waters TW1, 2, PW = pore water, and the superscripts 0 and ∞ denote the tracer concentrations prior to and after equilibration of the test water with the pore water.

The stable isotope composition of the pore water is calculated from mass balance relationship of the experiments according to:

$$C_{PW} = \frac{(M_{TW1} \cdot C_{TW1}^{\infty} \cdot C_{TW2}^0) + (M_{TW1} \cdot C_{TW1}^0 \cdot C_{TW2}^{\infty}) + (M_{TW2} \cdot C_{TW1}^{\infty} \cdot C_{TW2}^0) - (M_{TW2} \cdot C_{TW1}^0 \cdot C_{TW2}^{\infty})}{(M_{TW1} \cdot C_{TW1}^0) + (M_{TW2} \cdot C_{TW2}^{\infty}) - (M_{TW1} \cdot C_{TW1}^{\infty}) - (M_{TW2} \cdot C_{TW2}^0)} \quad (3)$$

where M = mass, C = isotope ratio, PW = pore water, TEW = test water, and the concentrations on the left side of the equation are prior to equilibration ($t = 0$), while the concentration on the right side is after equilibration is achieved ($t = \infty$) in the experiment. The two experiments deliver four equations of type (3) which are solved for the three unknown $\delta^{18}\text{OPW}$, $\delta^2\text{HPW}$ and M_{PW} .

The error of the calculated mass of pore water and pore-water isotope composition obtained from such type of experiments is mainly sensitive to the ratio of pore water to test water used as can be shown by applying Gauss' law of error propagation. To improve the error obtained in earlier studies on material from boreholes KFM06A /Waber and Smellie 2005/ and KLX03 /Waber and Smellie 2006/ larger masses of rock were used for the experiment in the three reservoir systems – rock sample, test water, and the air inside the container as a diaphragm.

Out-diffusion experiments were performed on complete core samples of about 120 mm to 190 mm in length by immersion into ultra-pure water (Figure 2-1). To accelerate the out-diffusion, the vapour-tight PVC containers were placed into a water bath with a constant temperature of 45°C . The weight of the core sample, the experiment container, and the artificial test water used was measured before and after the experiment to ensure that no loss of test water has occurred during the entire experiment. Weighing of the core before and after the experiment gives additional valuable information about the saturation state of the core at the beginning of the experiment.

At specific time intervals, initially a few days and later a few weeks, 0.5 mL of solution were sampled for the determination of the chloride concentration as a function of time. The small samples were analysed on a Metrohm 861 Compact ion-chromatograph. The analytical error of these determinations is about 5% based on multiple measurements of the standard solutions.

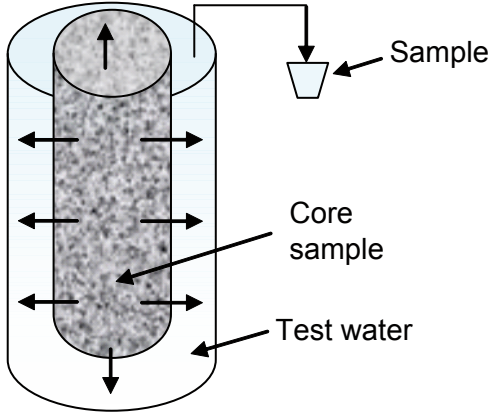


Figure 2-1. Schematic picture of out-diffusion experiments performed.

After equilibrium with respect to chloride was achieved, the core was removed from the container and the solution was immediately analysed for pH and alkalinity (by titration). The remaining solution was split into different aliquots for chemical and isotopic analyses. Major cations and anions were analysed by ion-chromatography with a relative error of 5% based on multiple measurements of standard solutions. Dissolved silicon was analysed by photometry with a relative error of 5%.

The chloride concentration of the experiment solution can be converted to pore water concentrations using mass balance calculations given that steady-state conditions in the out-diffusion experiment are achieved. At steady-state conditions the chloride concentration in the connected porosity of the rock sample will be equal to that of the experiment solution. With knowledge of the mass of pore water in the rock sample, the chloride concentration of the pore water can be calculated according to:

$$C_{PW} = \frac{\left(M_{PW} + M_{TEWi} - \sum^n M_S \right) \cdot C_{equil,corrected} - (M_{TEWi} \cdot C_{TEWi}) + \sum^n M_S \cdot C_S}{M_{PW}} \quad (4)$$

with:

$$C_{equil,corrected} = \frac{C_{TW\infty} \cdot \left(M_{TWi} - \sum^n M_S \right)}{M_{TWi}} \quad (5)$$

where C = concentration, M = mass, n = number of samples and the subscripts PW = pore water, TEW = experiment solution, S = small-sized sample taken for chloride time-series, i = at beginning of experiment, and ∞ = at end of experiment.

The last term in equation (4), $\sum M_S \cdot C_S$, describes the amount of chloride removed from the initial experiment solution by the chloride time-series samples. The final measured concentration of chloride in the experiment solution, $C_{TEW\infty}$, is corrected for the mass of solution removed by the chloride time-series samples from the initial mass of the experiment solution, M_{TEWi} , in order to obtain the Cl concentration in the experiment solution at steady state, $C_{equil,corrected}$ (equation 5). A correction for chloride in the initial experiment solution ($M_{TEWi} \cdot C_{TEWi}$) is necessary if this solution is not entirely free of chloride.

It should be noted that the unit of pore-water concentrations is given as mg/kg_{H₂O} (and not mg/L) because it is derived on a mass basis rather than a volumetric basis. This is because the density of the pore water is not known beforehand. In reality and within the overall uncertainty band, the difference between mg/kgH₂O and mg/L becomes only important at an ionic strength of the calculated pore water above that of sea water (~ 0.7 M) corresponding to a total mineralisation of ~35 g/L.

2.3 Data handling

Original data regarding the reported activities are stored in the primary Sicada database, in which they are traceable by the Activity Plan number (AP PF 400-05-116 or AP PF 400-05-117). Only data in the database are acceptable for further interpretation and modelling. The data presented in this report are regarded as copies of the original data. Data in the databases may be revised, if needed. Such revisions will not necessarily result in a revision of the P-report; minor revisions are normally presented as supplements, available at www.skb.se.

2.4 Nonconformities

All activities have been performed according to the Activity Plans except for the diffusive isotope equilibration performed on five samples of borehole KFM09B.

A failure of the temperature control in the cabinet used for the diffusive isotope equilibration experiments led to condensation of test and pore water on the walls of the vapour-tight glass containers in 10 out of the 16 containers. The analysed isotope values of these five samples show a clear deterioration induced by this condensation that can no longer be corrected for. Therefore, only three water contents and pore-water isotope compositions derived by this method are available for samples from borehole KFM09B.

3 KFM01D borehole: Pore-water data

Borehole KFM01D was drilled in the western part of the investigation area from November 22nd, 2005, to February 18th, 2006. The borehole was intended to deliver hydrogeological and hydrochemical information about the rock volume of the central part of a potential repository area and to confirm or otherwise the existence of gently-dipping brittle zones, among them ZFM61, that are suggested from modelling the seismic and other ground geophysical data of the area. Borehole KFM01D was drilled at an inclination of 55° towards the NE to a total length of 800.24 metres.

Between January 7th and February 17th 2006, a total of 14 samples were collected for pore-water characterisation at regular intervals of about 50 metres from a borehole length of 140 m downwards. Table 3-1 gives the list of samples used for pore-water characterisation including their SKB number, the sample numbering used in this report, and the experiments and analyses performed on each sample. The general rock type, the distance of the sample to the next proximate tectonised zone and the frequency of open fractures /from Petersson et al. 2006a/ in the near-vicinity of each sample are given in Table 3-2.

Table 3-1. KFM01D borehole: List of samples used for pore-water studies and experiments and measurements performed.

Sample no.	SKB sample no.	Average depth along borehole (m)	Average depth below surface (m) ¹⁾	Water loss porosity	Density	Diff. isotope equil. method	Out-diffusion experiments		
							Chemistry	⁸⁷ Sr/ ⁸⁶ Sr δ ³⁷ Cl	CI time-series
KFM01D-1	SKB 012108	140.69	115.25	X	X	X	X	P	X
KFM01D-2	SKB 012109	191.73	157.06	X	X	X	X	P	O
KFM01D-3	SKB 012110	255.13	208.99	X	X	X	X	P	O
KFM01D-4	SKB 012111	299.09	245.00	X	X	X	X	P	X
KFM01D-5	SKB 012112	352.07	288.40	X	X	X	X	P	X
KFM01D-6	SKB 012113	393.69	322.49	X	X	X	X	P	X
KFM01D-7	SKB 012114	462.79	379.09	X	X	X	X	P	X
KFM01D-8	SKB 012115	500.05	409.62	X	X	X	X	P	X
KFM01D-9	SKB 012116	544.23	445.81	X	X	X	X	P	O
KFM01D-10	SKB 012117	600.25	491.69	X	X	X	X	P	X
KFM01D-11	SKB 012118	643.12	526.81	X	X	X	X	P	X
KFM01D-12	SKB 012121	700.25	573.61	X	X	X	X	P	X
KFM01D-13	SKB 012122	747.29	612.14	X	X	X	X	P	X
KFM01D-14	SKB 012124	790.56	647.58	X	X	X	X	P	X

¹⁾ borehole inclination: 55°,

X = experiment performed, analytical data available,

P = experiment performed, analytical data pending,

O = experiment performed, analytical data not completed due to leakage of small-sized sample device.

Table 3-2. KFM01D borehole: Sample geology and distance to fractures.

Sample no.	Average depth along borehole (m)	Lithology	Alteration/ tectonisation ¹⁾	Fracture intensity ¹⁾
KFM01D-1	140.69	metagranite, homog. medium-grained, white-grey	± 5 m	high
KFM01D-2	191.73	metagranite, homog. medium-grained, white-grey	± 5 m	high
KFM01D-3	255.13	metagranite, homog. fine-grained, foliated, white-grey	± 5 m	low
KFM01D-4	299.09	metagranite, homog. medium-grained, white-grey	± 5 m	low
KFM01D-5	352.07	metagranite, homog. fine to med.-grained, white-grey	± 5 m	moderate
KFM01D-6	393.69	metagranite, homog. fine-grained, foliated, white-grey	± 5 m	moderate
KFM01D-7	462.79	metagranite, homog. med-grained, foliated, white-grey	± 5 m	low
KFM01D-8	500.05	metagranite, porphyric med.-grained, foliated, grey	± 5 m	low
KFM01D-9	544.23	metagranite, porphyric med.-grained, foliated, grey	± 25 m	low
KFM01D-10	600.25	metagranite, homog. med.-grained, white-grey	± 25 m	low
KFM01D-11	643.12	metagranite, porphyric medium-grained, foliated, grey	± 40 m	low
KFM01D-12	700.25	granodiorite, homog. med.-grained, foliated, red-grey	± 5 m	moderate
KFM01D-13	747.29	pegmatitic granite, homog. med.-grained, dark grey	± 20 m	low
KFM01D-14	790.56	metagranite, homog. med-grained, foliated, dark grey	± 20 m	low

¹⁾ approximate distance to next major alteration zone and fracture intensity above and below sample (from WellCAD image, /Petersson et al. 2006a/).

The dominant rock type encountered in borehole KFM01D is a metagranite which locally becomes slightly granodioritic in composition /Petersson et al. 2006a/. In the drillcore the metagranite is mainly fine-grained from 191–499 metres and more medium-grained further downwards. The second most common rock type is a pegmatitic granite which occurs in sections of commonly less than 2 metres thickness, but constitutes about 20% of the entire drillcore. Subordinate in occurrence are fine- to medium-grained metagranitoids of granitic to granodioritic composition and amphibolites. All rocks have experienced Svecofennian metamorphism under amphibolite facies conditions /Petersson et al. 2006a/. Rock foliation is frequently developed leading to a distinct anisotropy and to a gneissic appearance of certain core sections. Tectonisation, rock alteration and frequency of open fractures are high in the first about 200 m of the drillcore, after which they decrease continuously with increasing depth. Below about 400 m open fractures are limited and occur only in a few tectonised zones at about 490 m, 690 m, and 770 m borehole lengths.

In open fractures calcite, epidote and chlorite are the most abundant minerals over the entire core lengths /Petersson et al. 2006a/. Pyrite occurs only rarely, while oxidised iron phases (hematite, iron hydroxides) are present throughout and are abundant in the three tectonised zones at about 490 m, 690 m, and 770 m depth along the borehole lengths.

From differential flow logging of borehole KFM01D an accumulation of highly transmissive fractures (up to 10^{-5} m²/s) was observed between 100–200 m borehole length /Väisävaara et al. 2006a/. At greater depth the transmissivity of the fractures decreases and below 550 m a measurable transmissivity could be determined only for one open fracture.

3.1 Water content and water-loss porosity

The water content of most samples investigated from borehole KFM01D falls within the narrow range of 0.08–0.12 wt.% (Table 3-3). A larger range of the water content is observed in the first 450 m of the drillcore, after which it decreases constantly from 500 m to the end of the borehole. For most samples there is good agreement in the water content derived by the two independent methods, i.e. by drying at 105°C to stable weight conditions (WC_{Drying}) and by the diffusive isotope equilibration method (WC_{IsoExch}), within the uncertainty band (Figure 3-1). This accounts especially for those samples where WC_{Dry} represents an average value of four sub-samples including the large-sized sample used for the out-diffusion experiment. In turn, larger differences are obtained for those samples with only one gravimetric water-loss measurement available and samples from more tectonised and/or oxidised zones (see below). This highlights once more the strong dependency of WC_{Dry} on the sample's textural homogeneity and mass, and the influence of clay minerals and hydroxides on WC_{IsoExch} , respectively.

Two samples (KFM01D-4 and KFM01D-7) revealed considerably higher water contents than the others (Table 3-3). Both these samples come from areas with a frequency of small-sized pegmatitic zones and have undergone more intense alteration. Together with sample KFM01D-1 these samples display a higher water content derived by drying compared to that derived by the diffusive isotope equilibration method. This suggests differences in mineralogy, more specifically in the contents of secondary minerals such as zeolites and hydroxides, which might partly loose bound water during drying at 105°C over extended periods of time and thus perturb the measured weight loss.

Table 3-3. KFM01D borehole: Water content derived by drying at 105°C and by the diffusive isotope equilibration method.

Laboratory sample no.	Borehole length (m)	Number of samples	Water content by drying at 105°C		Water content by diffusive isotope equilibration method	
			average (wt.%)	1 σ (wt.%)	(wt.%)	error ¹⁾ (wt.%)
KFM01D-1	140.69	2	0.119	0.013	0.101	0.008
KFM01D-2	191.73	2	0.087	0.003	0.109	0.007
KFM01D-3	255.13	4	0.082	0.005	0.114	0.007
KFM01D-4	299.09	1 ²⁾	0.147	0.015	0.112	0.007
KFM01D-5	352.07	1 ²⁾	0.105	0.011	0.128	0.008
KFM01D-6	393.69	1 ²⁾	0.100	0.010	0.121	0.007
KFM01D-7	462.79	1 ²⁾	0.186	0.019	0.152	0.007
KFM01D-8	500.05	4	0.125	0.003	0.133	0.009
KFM01D-9	544.23	1 ²⁾	0.097	0.010	0.139	0.008
KFM01D-10	600.25	1 ²⁾	0.131	0.013	0.123	0.007
KFM01D-11	643.12	4	0.123	0.013	0.122	0.007
KFM01D-12	700.25	4	0.125	0.028	0.129	0.007
KFM01D-13	747.29	4	0.107	0.001	0.102	0.006
KFM01D-14	790.56	4	0.112	0.015	0.104	0.005

¹⁾ error calculated with Gauss' law of error propagation,

²⁾ assumed error \pm 10%.

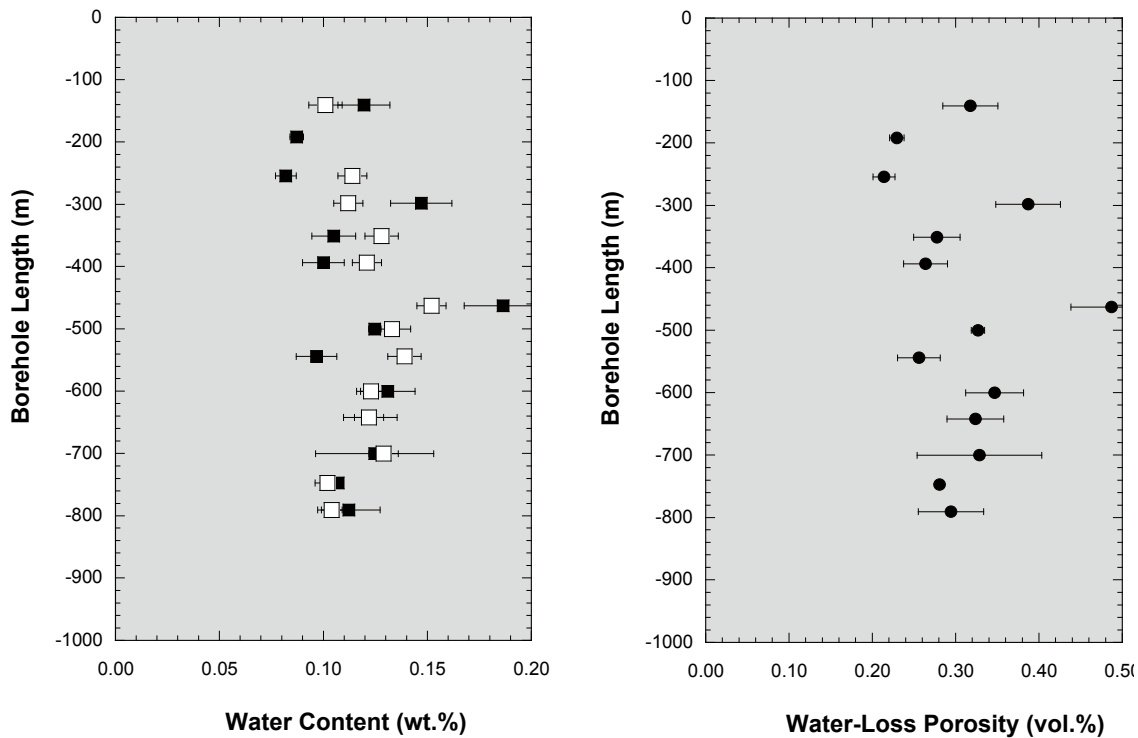


Figure 3-1. Borehole KFM01D: Water content derived by drying at 105°C to stable weight (left, closed symbols) and by the diffusive isotope equilibration method (left, open symbols), and the water-loss porosity of metagranite samples as a function of the borehole length (right).

Modifications of the true water content induced by re-saturation are observed for those samples where only one single measurement of drying to stable weight conditions is listed in Table 3-3. Because of a shortage in free space in the ovens used for drying, these samples had to be stored for about 2 months before the drying process could be started. Vapour-tight containers at 100% humidity were used for storage. Interestingly, the measured weight loss of all samples stored in this way was more than twice as high compared to that of the reference sample. This is due to sorption and condensation of water from the air in the containers on the fresh rock surfaces and in the newly created pore space (by stress release) during storage. The induced strong perturbation of the true water content highlights once more the difficulties attached to re-saturation techniques often applied for water content and water-loss porosity measurements. Because these measurements do not represent in situ conditions, they were not further used.

In summary, the water contents of KFM01D samples are small and fall within a narrow range with a larger spread in the data along the first 450 m of the drillcore. Below 500 m borehole length the water content systematically decreases with increasing borehole length to values around 0.1 wt.%. The same trends are observed for the water-loss porosity (WL-porosity; Figure 3-1), calculated from the water content derived by drying and the density obtained from mass and volumetric measurements of the large-scale samples (approx. 1 kg) used for the out-diffusion experiments (Table 3-4). The depth distribution obtained for water content and WL-porosity in borehole KFM01D coincides well with that of the P-wave velocity obtained in borehole KFM01A drilled from the same location, where also a general decrease from 500 m downwards was obtained /Tunbridge and Panayiotis 2003/.

Table 3-4. KFM01D borehole: Bulk density and water-loss porosity.

Laboratory sample no.	Borehole length (m)	Number of samples	Bulk density (wet) ¹⁾ (g/cm ³)	Water-loss porosity	
				average (vol.%)	1 σ (vol.%)
KFM01D-1	140.69	2	2.664	0.32	0.03
KFM01D-2	191.73	2	2.635	0.23	0.01
KFM01D-3	255.13	4	2.616	0.21	0.01
KFM01D-4	299.09	1 ²⁾	2.638	0.39	0.04
KFM01D-5	352.07	1 ²⁾	2.648	0.28	0.03
KFM01D-6	393.69	1 ²⁾	2.645	0.26	0.03
KFM01D-7	462.79	1 ²⁾	2.621	0.49	0.05
KFM01D-8	500.05	4	2.624	0.33	0.01
KFM01D-9	544.23	1 ²⁾	2.653	0.26	0.03
KFM01D-10	600.25	1 ²⁾	2.653	0.35	0.04
KFM01D-11	643.12	4	2.646	0.32	0.03
KFM01D-12	700.25	4	2.642	0.33	0.08
KFM01D-13	747.29	4	2.626	0.28	0.01
KFM01D-14	790.56	4	2.628	0.30	0.04

¹⁾ determined from mass and volume of saturated (wet) drillcore sample used for out-diffusion experiment,

²⁾ assumed error \pm 10%.

3.2 Out-diffusion experiments

Out-diffusion experiments have been performed on 14 core samples from borehole KFM01D. The samples were collected on-site from fracture-free rock portions with the most proximate open and/or closed fracture being some 5 m away if possible. For 10 samples enough material was received to perform the out-diffusion experiment on a fracture-free core sample of 19 cm length, i.e. on a rock mass of about 1 kg. For 4 samples (KFM01D-4, 5, 9 and 10) a 12 cm long core piece (approx. 0.6 kg of rock) was used for the experiments. In all experiments the weight ratio of test water to rock was kept between about 0.105 and 0.134 and the experiment temperature was 45°C (Table 3-5).

3.2.1 Equilibrium control in the out-diffusion experiment

The monitoring of steady-state conditions in the out-diffusion experiments was performed with small-sized samples of 0.5 mL that were taken at regular intervals and analysed for their anion concentration. Equilibrium conditions with respect to chloride concentrations in the remnant solution in the pore volume of the rock and the test water in the sample container is attained when the Cl time-series concentrations reach a plateau, i.e. when they remain constant. With respect to the out-diffusion of chloride, equilibrium conditions have been attained in the experiments after about 50 to 60 days independent of the samples mass, porosity or depth of sampling (Figure 3-2). To allow a complete equilibration the experiment time has been fixed for all samples to 105 days based on previous experience.

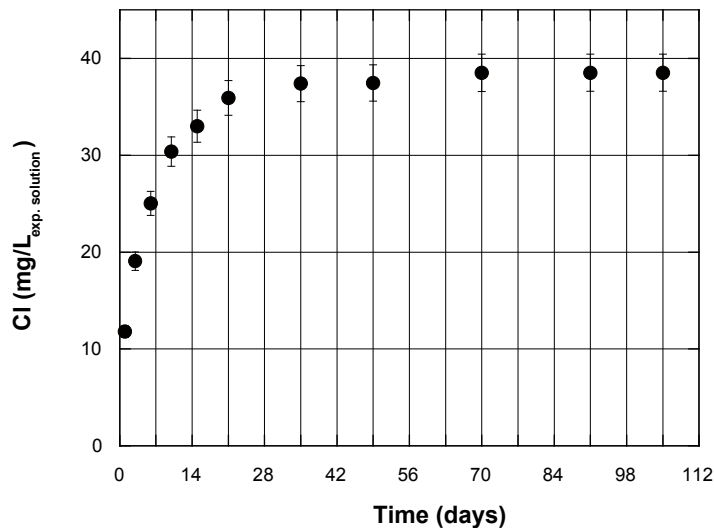


Figure 3-2. Borehole KFM01D: Example of chloride time-series displaying that steady-state conditions in the out-diffusion experiments have been achieved after about 50 days (sample KFM01D-7, vertical depth below surface = 379.09 m, $\Phi_{WL} = 0.49$ vol.%).

3.2.2 Chemical composition of experiment solution

The chemical composition of the supernatant solution after termination of the out-diffusion experiments is given in Table 3-5.

The pH of the experiment solutions varied between 6.22 and 7.13 and the total mineralisation ranged from 156 mg/L to 262 mg/L. It should be noted that the total mineralisation obtained for the experiment solution is dependent on the water content of the sample and does not directly reflect differences in pore-water salinity. During the experiment, mineral dissolution obviously will affect the concentrations of reactive compounds, pH and total mineralisation so that these are not representative for in situ pore water. Major reactions that affect measured elemental concentrations in the experiment solutions involve the dissolution of plagioclase (Ca, Na), K-feldspar (K), biotite (K, Mg), muscovite (K), chlorite (Mg) and possibly fluorite (F), pyrite (SO₄) and calcite (Ca, CO₃). The dissolution of Al-silicate minerals consumes carbonic acid present in the initial test water and will also change the total alkalinity of the test water. Because the general rock mineralogy is rather constant over the entire drillcore, mineral dissolution during the experiments is expected to be similarly uniform. Preliminary results of geochemical model calculations including mineral dissolution kinetics show that the contribution from mineral dissolution will not significantly alter the general chemical type of the experiment solutions, except for dissolved carbonate. With these exceptions, the chemical type determined on the basis of the experiment solution is qualitatively acceptable as being that of the in situ pore water.

The chemical character of the experiment solutions is fairly similar for most samples and represents a Na-Ca-HCO₃-Cl type. Towards the end of the borehole the chemistry changes to a Na-Ca-Cl-HCO₃ type. Compositional differences are restricted to the ratios of alkaline earth elements (Ca, Mg, Sr) to Na and that of Cl to the total alkalinity, both of which are generally increasing with increasing depth (Figure 3-3). To what degree bicarbonate (HCO₃⁻) forms part of the chemical type of the in situ pore water is currently difficult to judge as outlined below.

Table 3-5. Chemical composition of solutions from out-diffusion experiments at steady-state conditions.

Out-diffusion experiment	solution	Units	KFM01D-1	KFM01D-2	KFM01D-3	KFM01D-4	KFM01D-5	KFM01D-6	KFM01D-7	KFM01D-8
SAMPLE DESCRIPTION										
Borehole length		m	140.69	191.73	255.15	298.09	351.07	393.69	462.77	500.05
Rock type			granite	granite	fine-grained granite	granite	granite	granite	granite	orthogneiss
Water-rock ratio			0.105	0.108	0.110	0.134	0.123	0.108	0.115	0.116
Experiment temperature		°C	45	45	45	45	45	45	45	45
Experiment time		days	105	105	105	105	105	105	105	105
MISC. PROPERTIES										
Chemical type			$\frac{\text{Na-Ca-}}{\text{HCO}_3\text{-Cl}}$	$\frac{\text{Na-Ca-}}{\text{HCO}_3\text{-Cl-(F)}}$	$\frac{\text{Na-Ca-Cl-}}{\text{HCO}_3}$	$\frac{\text{Ca-Na-}}{\text{HCO}_3\text{-Cl}}$	$\frac{\text{Na-Ca-}}{\text{HCO}_3\text{-Cl-(F)}}$	$\frac{\text{Na-Ca-}}{\text{HCO}_3\text{-Cl-(F)}}$	$\frac{\text{Na-Ca-}}{\text{HCO}_3\text{-Cl}}$	$\frac{\text{Na-Ca-}}{\text{HCO}_3\text{-Cl}}$
pH (lab)			6.90	6.54	6.22	6.84	6.99	6.97	6.99	6.64
Electrical conductivity										
Sample temperature		°C	20	20	20	20	20	20	20	20
CATIONS										
Sodium (Na ⁺)		mg/L	38.8	30.5	28.2	27.5	30.0	43.9	47.1	40.2
Potassium (K ⁺)		mg/L	2.3	2.2	2.0	2.7	1.5	2.0	1.7	2.7
Magnesium (Mg ⁺²)		mg/L	< 0.5	< 0.5	< 0.5	< 0.5	< 0.5	< 0.5	< 0.5	< 0.5
Calcium (Ca ⁺²)		mg/L	28.0	17.7	22.6	32.8	16.3	9.7	30.5	15.0
Strontium (Sr ⁺²)		mg/L	< 0.5	< 0.5	< 0.5	< 0.5	< 0.5	< 0.5	< 0.5	< 0.5
ANIONS										
Fluoride (F ⁻)		mg/L	4.0	4.4	3.3	2.2	4.3	5.1	1.9	3.5
Chloride (Cl ⁻)		mg/L	32.2	18.8	30.8	29.9	28.3	27.0	38.7	28.2
Bromide (Br ⁻)		mg/L	0.6	< 0.5	< 0.5	< 0.5	< 0.5	< 0.5	0.7	< 0.5
Sulphate (SO ₄ ⁻²)		mg/L	5.4	6.9	8.1	4.2	3.4	5.4	14.1	6.8
Nitrate (NO ₃ ⁻)		mg/L	4.9	3.5	10.2	3.6	5.6	0.7	< 0.5	0.8
Total alkalinity		meq/L	1.47	1.00	0.75	1.5	0.9	1.13	1.86	1.22
NEUTRAL SPECIES										
Silica (Si)		mg/L	11.90	16.20	7.07	10.30	10.90	15.40	13.70	15.20
CALC. PARAMETERS										
Total dissolved solids		mg/L	218	162	159	206	156	179	262	188
Charge balance		%	6.59	7.51	6.26	5.48	1.57	3.39	4.14	4.78

Table 3-5. (continued)

Out-diffusion experiment solution	Units	KFM01D-9	KFM01D-10	KFM01D-11	KFM01D-12	KFM01D-13	KFM01D-14	Blank solution
SAMPLE DESCRIPTION								
Borehole length	m	544.23	600.24	643.31	700.25	723.75	790.56	
Rock type		granite	granite	orthogneiss	granite	granite	granite	
Water-rock ratio		0.132	0.126	0.113	0.112	0.114	0.114	
Experiment temperature	°C	45	45	45	45	45	45	
Experiment time	days	105	105	105	105	105	106	
MISC. PROPERTIES								
Chemical type		Na-Ca- $\frac{\text{HCO}_3\text{-Cl}}{\text{HCO}_3\text{-Cl}}$	Na-Ca- $\frac{\text{HCO}_3\text{-Cl-(F)}}{\text{HCO}_3\text{-Cl-(F)}}$	Na-Ca- $\frac{\text{HCO}_3\text{-Cl}}{\text{HCO}_3\text{-Cl}}$	Na-Ca- $\frac{\text{HCO}_3\text{-Cl}}{\text{HCO}_3\text{-Cl}}$	Na-Ca- $\frac{\text{HCO}_3\text{-Cl}}{\text{HCO}_3\text{-Cl}}$	Na-Ca-Cl- $\frac{\text{HCO}_3}{\text{HCO}_3}$	
pH (lab)	$-\log(\text{H}^+)$	6.89	7.13	7.08	6.86	7.07	6.92	
Electrical conductivity	$\mu\text{S/cm}$	20	20	20	20	20	20	< 10
Sample temperature	°C	20	20	20	20	20	20	20
CATIONS								
Sodium (Na ⁺)	mg/L	34.6	37.6	33.1	46.2	38.4	38.6	< 0.1
Potassium (K ⁺)	mg/L	4.1	2.2	1.9	3.7	4.2	3.7	< 0.1
Magnesium (Mg ⁺²)	mg/L	0.5	< 0.5	< 0.5	< 0.5	< 0.5	< 0.5	< 0.5
Calcium (Ca ⁺²)	mg/L	22.3	18.0	20.6	22.5	23.5	30.8	< 0.5
Strontium (Sr ⁺²)	mg/L	< 0.5	< 0.5	< 0.5	< 0.5	< 0.5	< 0.5	< 0.5
ANIONS								
Fluoride (F ⁻)	mg/L	3.7	4.5	3.9	3.8	4.7	3.4	< 0.5
Chloride (Cl ⁻)	mg/L	23.9	24.4	32.3	33.6	39.3	56.3	< 0.1
Bromide (Br ⁻)	mg/L	< 0.5	< 0.5	< 0.5	< 0.5	0.6	0.7	< 0.5
Sulphate (SO ₄ ⁻²)	mg/L	6.1	3.0	6.2	2.0	7.7	6.3	< 0.5
Nitrate (NO ₃ ⁻)	mg/L	< 0.5	2.9	1.9	4.2	< 0.5	7.9	< 0.5
Total alkalinity	meq/L	1.44	1.35	1.16	1.46	1.32	1.09	< 0.1
NEUTRAL SPECIES								
Silica (Si)	mg/L	13.50	9.99	8.43	9.83	10.80	12.30	< 0.01
CALC. PARAMETERS								
Total dissolved solids	mg/L	197	185	179	215	210	226	< 1.0
Charge balance	%	6.17	4.07	1.41	8.50	2.13	3.04	-

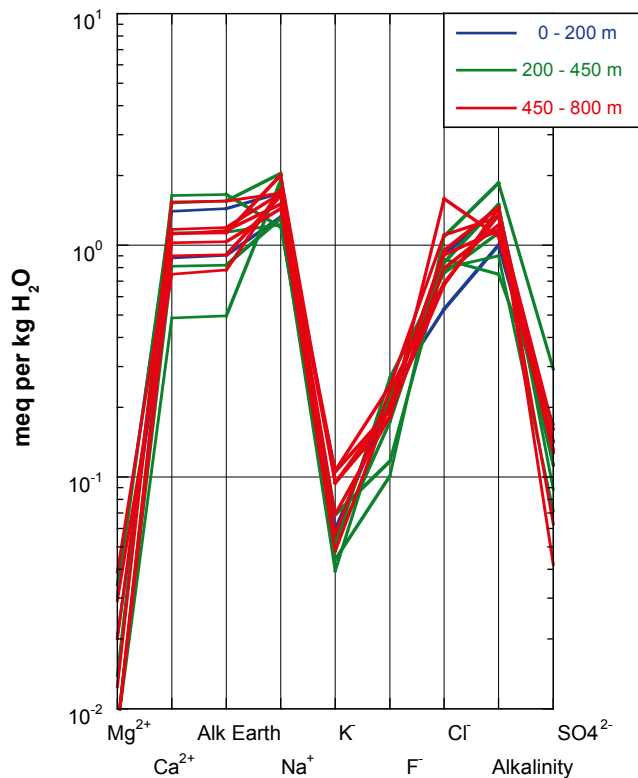


Figure 3-3. Borehole KFM01D: Schoeller diagram of experiment solutions from the drillcore samples showing the change in chemical type and degree of mineralisation as a function of the differently transmissive depth intervals (cf Figure 3-4).

Dissolved carbonate in the experiment solution, here expressed as bicarbonate (HCO_3^-), has occurred to some degree prior to the experiment because it was in equilibrium with atmospheric pCO_2 ($\log \text{pCO}_2 \sim -3.5$). However, the measured total alkalinity and the total carbon concentration calculated from that in the solutions at the end of the experiments are significantly higher than that initially present in the test water. A possible origin of large amounts of carbon through contamination by the experiment set-up is not indicated because the blank experiment remained essentially at atmospheric total carbon. This suggests that the carbon source(s) are the pore water itself and carbon-providing mineral dissolution reactions. Geochemical model calculations show that at the measured conditions all experiment solutions are under-saturated with respect to calcite at corresponding high partial pressures of CO_2 ($\log \text{pCO}_2$ of around -2). Together with the low abundance of carbonate minerals in the rock this suggests that mineral carbonate is only a minor source of carbon in this system. Thus, most of the dissolved carbon appears to originate from the pore water where it presumably occurs mainly in the oxidised state (HCO_3^- , CO_3^{2-}). In most experiments an increase in pressure in the experiment device was observed during the first days, suggesting that degassing of pressurised gas such as dissolved CO_2 occurred in the initial stages of the experiment. Besides the carbonate dissolution reactions, this inhibits the direct comparison of the measured carbonate system parameters to those present under in situ conditions. In addition, there are also indications that reduced hydrocarbons (e.g. CH_4) might be present in the pore water. This comes from the observation of a faint smell of H_2S in several sample containers, which could indicate that minor sulphate reduction by microbes utilising reduced hydrocarbons could have taken place during the experiment.

3.2.3 Implications for pore-water composition

Chemically conservative elements such as Cl and Br are not affected by mineral dissolution because there are no Cl- and Br-bearing minerals present in the rock. Other sources for these elements such as fluid inclusion leakage can also be excluded due to the non-destructive design of the experiment as discussed in detail in /Waber and Smellie 2006, 2007/. Therefore the concentrations of these compounds can be converted to in situ pore-water concentrations using the mass balance calculation given in equation (4) and as is shown below in Section 3.3.

In borehole KFM01D no correlation is established between the chemical type of the experiment solution and fracture frequency distribution in the borehole over the first 700 m of borehole length (Figure 3-3). This contrasts to observations made in borehole KFM06A where such a correlation is established /Waber and Smellie 2005/. The difference appears to be related to the overall less transmissive character of the bedrock encountered in borehole KFM01D, thus maintaining a more homogeneous pore-water composition also at shallower depths. A change in the chemical type of the pore water is only indicated towards the end of the borehole in the very low transmissive section below about 700 m borehole length (about 573 m vertical depth below surface).

The chemical composition therefore indicates that the pore water in the metagranite of borehole KFM01D is of a general Na-Ca-Cl-HCO₃⁻ type with the importance of the bicarbonate being yet undefined. Sulphate concentrations appear to be rather low, but there are indications that dissolved sulphur and also dissolved carbon occur in the in situ pore water in the oxidised and reduced state(s).

3.3 Chloride composition of pore-water

Calculated pore-water chloride concentrations in the rock matrix of borehole KFM01D are mainly in the range of 2–3 g/kgH₂O down to about 600 m borehole length (approx. 573 m vertical depth below surface; Figure 3-4). Exceptions are three samples at 255 m, 352 m and 544 m borehole length which have Cl concentrations up to 4 g/kgH₂O. These samples are located outside the more transmissive parts from 100–200 m and 300–420 m borehole length, but are associated with less transmissive fractures (Figure 3-4). Below 600 m the pore-water chloride concentration steadily increases to 5.7 g/L towards the end of the borehole at 790 m borehole length (approx. 647 m vertical depth).

The sensitivity of the calculated pore-water Cl concentration depends essentially on the accuracy of the determination of the mass of pore water because of its inverse proportionality to the mass of pore water. As discussed above, the mass of pore water derived from water-content measurements may be influenced by various perturbations which can result in a deviation of the measured water-content value from that present in situ. As discussed in detail by /Waber and Smellie 2007/ the sample handling and methods applied here to derive the water content, the independency of the methods and the good agreement of the data, indicate that neither stress release nor de-saturation had a significant effect on the present measurements and that the measured values are representative for in situ conditions. The uncertainty band of the calculated Cl concentration of the pore water is therefore mainly given by the standard deviation of the multiple water-content measurements.

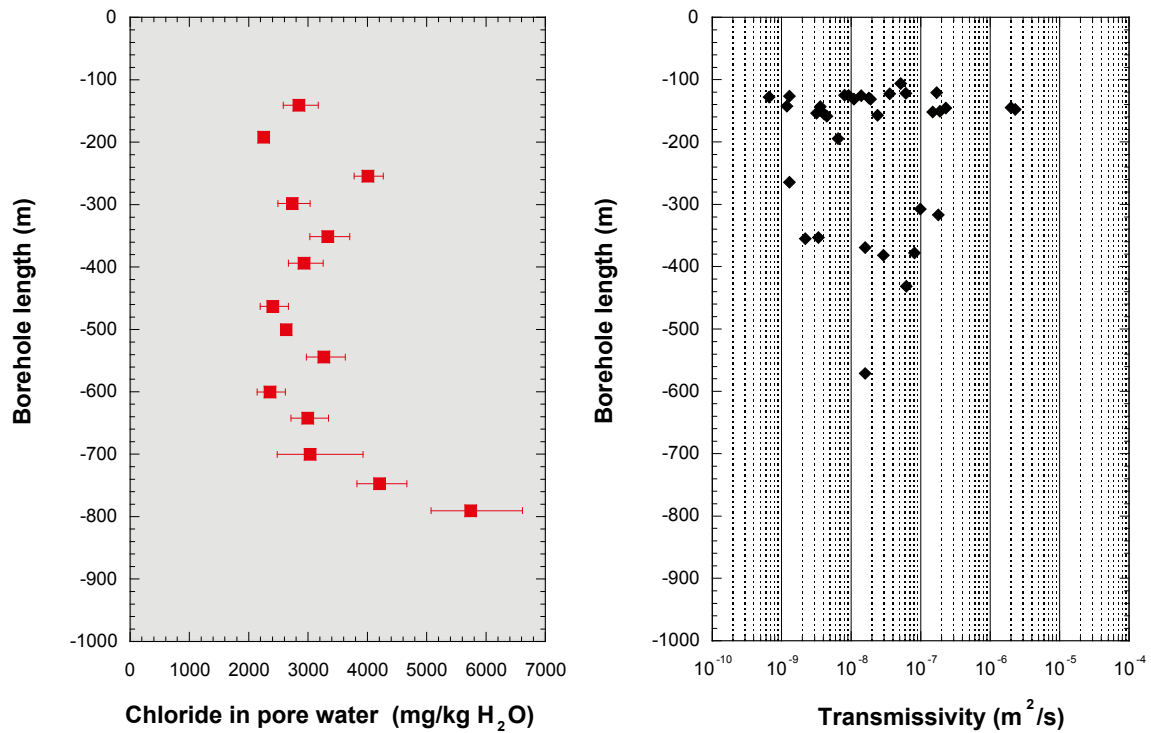


Figure 3-4. Borehole KFM01D: Chloride concentration of pore water as a function of sampling depth (left) compared to the measured hydraulic transmissivity of all detected fractures (right, data from Väisäsvaara et al. 2006a/).

Table 3-6. KFM01D borehole: Chloride concentration of pore water.

Laboratory sample no.	Borehole length (m)	Lithology	Pore water Cl (mg/kg H ₂ O)	Pore water Cl + error ¹⁾ (mg/kg H ₂ O)	Pore water Cl - error ¹⁾ (mg/kg H ₂ O)
KFM01D-1	140.69	med.-grain. granite	2,846	328	266
KFM01D-2	191.73	fine-grained granite	2,251	89	82
KFM01D-3	255.13	fine-grained granite	4,008	260	230
KFM01D-4	299.09	fine-grained granite	2,736	301	246
KFM01D-5	352.07	fine-grained granite	3,334	367	301
KFM01D-6	393.69	fine-grained granite	2,933	323	264
KFM01D-7	462.79	fine-grained granite	2,406	263	215
KFM01D-8	500.05	med.-grain. granite	2,634	65	62
KFM01D-9	544.23	med.-grain. granite	3,267	360	295
KFM01D-10	600.25	med.-grain. granite	2,356	259	212
KFM01D-11	643.12	med.-grain. granite	2,997	349	282
KFM01D-12	700.25	med.-grain. granite	3,038	887	558
KFM01D-13	747.29	med.-grain. granite	4,204	463	379
KFM01D-14	790.56	med.-grain. granite	5,743	875	669

¹⁾ error based on the standard deviation of multiple water-loss measurements.

3.4 Water-isotope composition of pore-water

The isotopic composition of the pore water was derived from the diffusive isotope equilibration technique. The error of the $\delta^{18}\text{O}$ and $\delta^2\text{H}$ values depends to a large degree on the ratio of the mass of pore water to the mass of test water used in the experiments. Unfortunately, for the samples of borehole KFM01D the error remained about the same as for the samples of borehole KFM06A /Waber and Smellie 2005/ and could not be reduced as initially planned due to the smaller amount of sample material received and by the fixed test water volume required for the mass spectrometric measurement.

Nevertheless, the derived $\delta^{18}\text{O}$ and $\delta^2\text{H}$ values allow some statements about the isotopic composition of the pore water as shown in Figure 3-5 where it is compared with the Global Meteoric Water Line (GMWL) and proposed end-member compositions of various groundwater types characterising the Forsmark area /Laaksoharju et al. 1999/. Most of the pore-water samples have an isotopic composition that plots within a narrow range on the right of the GMWL. They have $\delta^2\text{H}$ values that cover the range from the “Altered Sea” reference water to that of “Littorina” sea water, with some of the pore-water samples being more enriched in ^{18}O than these reference waters. The shallowest sample (KFM01D-1) and the deepest sample (KFM01D-14) are outside this group. The shallowest sample has a $\delta^2\text{H}$ value similar to that of the “Meteoric” reference water, but is also enriched in ^{18}O . The deepest sample plots on the GMWL, but is enriched in ^{18}O and ^2H compared to all reference waters (Figure 3-5).

To some degree, the isotope composition of the pore water also shows a depth dependency. Three groups of pore water are indicated with increasing depth (Figure 3-6). Down to 300 m borehole length the pore water has the most negative $\delta^{18}\text{O}$ values between -5‰ and -6.5‰ associated with rather high $\delta^2\text{H}$ values (-46‰ to -77‰). Between 300–600 m borehole length the $\delta^{18}\text{O}$ values are most enriched in ^{18}O (-2‰ to -4‰) and associated with the most negative

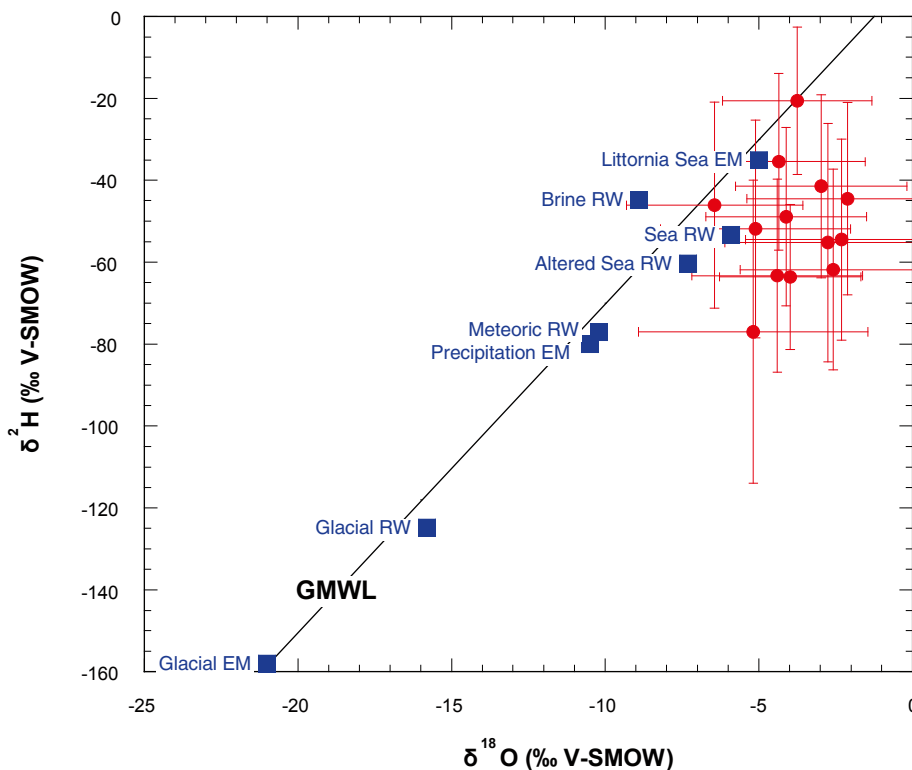


Figure 3-5. Borehole KFM01D: $\delta^{18}\text{O}$ and $\delta^2\text{H}$ values of pore water compared to the GMWL and the isotopic composition of proposed end-members (EM) and reference water (RW) compositions of various Swedish groundwaters (data from /Laaksoharju et al. 1999/). Error bars indicate cumulated error calculated with Gauss' law of error propagation.

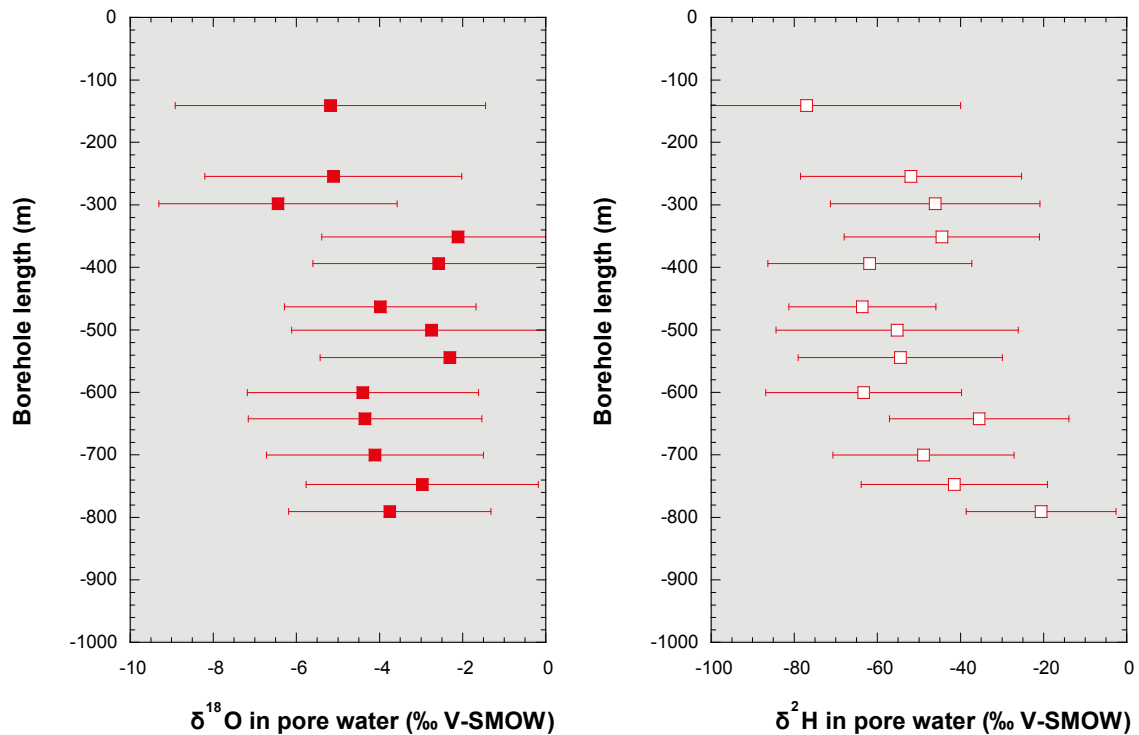


Figure 3-6. Borehole KFM01D: Depth variation of $\delta^{18}\text{O}$ and $\delta^2\text{H}$ in pore water. Error bars indicate cumulated error calculated with Gauss' law of error propagation.

$\delta^2\text{H}$ values (-45‰ to -64‰). From there down to the deepest sample at 790 m along the borehole (647 m depth below surface), the $\delta^{18}\text{O}$ values are again more negative between -3‰ and -4.4‰ associated with $\delta^2\text{H}$ values most enriched in ^2H (-20‰ to -49‰).

Table 3-7. KFM01D borehole: $\delta^{18}\text{O}$ and $\delta^2\text{H}$ of pore water.

Laboratory sample no.	Borehole length (m)	$\delta^{18}\text{O}^{(1)}$ pore water (‰ V-SMOW)	Absolute error $\delta^{18}\text{O}^{(1)}$ (‰ V-SMOW)	$\delta^2\text{H}^{(1)}$ pore water (‰ V-SMOW)	Absolute error $\delta^2\text{H}^{(1)}$ (‰ V-SMOW)
KFM01D-1	140.69	-5.18	3.7	-77.0	37.0
KFM01D-2	191.73	- ²⁾		- ²⁾	
KFM01D-3	255.13	-5.11	3.1	-51.9	26.6
KFM01D-4	299.09	-6.44	2.9	-46.1	25.2
KFM01D-5	352.07	-2.11	3.3	-44.5	23.5
KFM01D-6	393.69	-2.58	3.0	-61.8	24.5
KFM01D-7	462.79	-3.98	2.3	-63.6	17.7
KFM01D-8	500.05	-2.75	3.4	-55.2	29.1
KFM01D-9	544.23	-2.31	3.1	-54.5	24.6
KFM01D-10	600.25	-4.40	2.8	-63.3	23.5
KFM01D-11	643.12	-4.35	2.8	-35.5	21.6
KFM01D-12	700.25	-4.11	2.6	-48.9	21.8
KFM01D-13	747.29	-2.97	2.8	-41.5	22.4
KFM01D-14	790.56	-3.75	2.4	-20.6	18.0

¹⁾ error calculated with Gauss' law of error propagation,

²⁾ incorrect analysis due to evaporation.

4 KFM08C borehole: Pore-water data

Borehole KFM08C was drilled in the northern part of the investigation area at the western shore of Asphällsfjärden (Figure 1-1) from April 14th, 2005, to May 9th, 2006 with a break between April 26th, 2005, and January 30th, 2006. The borehole was drilled in the northeastern part of the candidate site, close to the western shore of Asphällsfjärden to provide hydrogeological information from expected repository depths close to the boundary of the site investigation area. Initially it was intended also to carry out hydrochemical characterisation of the borehole, but this was suspended because of a lack of suitable sampling locations. Borehole KFM08C was drilled at an inclination of 60° towards the NE under the Baltic Sea and to a total length of 951.1 metres.

Between February 6th and May 8th, 2006, a total of 10 samples were collected for pore-water characterisation at regular intervals of about 100 metres from a borehole length of 154 m downwards. Table 4-1 gives the list of samples used for pore-water characterisation including their SKB number, the sample numbering used in this report, and the experiments and analyses performed on each sample. The general rock type, the distance of the sample to the next proximate tectonised zone, and the frequency of open fractures /from Petersson et al. 2006b/ in the near-vicinity of each sample, are given in Table 4-2.

The dominant rock type encountered in borehole KFM08C is a medium-grained metagranite of greyish-red to grey in colour, similar to that found in other deep boreholes from the site /Petersson et al. 2006b/. Other rock types that commonly occur only over a few metres along the drillcore include pegmatitic granites, fine- to medium-grained metagranitoids, and a few amphibolite dykes. Rock foliation is well developed producing a distinct anisotropy and a gneissic appearance to some of the core sections. More intense ductile and brittle ductile deformation has also been observed in 27 zones along the drillcore with most of them being parallel to the rock foliation and being less than one decimetre in width /Petersson et al. 2006b/. All rocks have experienced Svecofennian metamorphism under amphibolite conditions and exhibit various degrees of alteration. Most prominent is an oxidation of the rock related to fracture concentrations down to about 700 m and an albitisation of the rocks between 342.2–546.5 m and again between 603.5–616.8 m borehole length /Petersson et al. 2006b/. The oxidation is apparent as a more or less strong haematite pigmentation of the feldspar grains. The albitisation is characterised by a bleached appearance and the occurrence of hornblende instead of biotite as the most abundant ferromagnesian phase, the latter predominating elsewhere in the metagranites. In such altered zones the recognition of the protolith is difficult to impossible to ascertain. Between 455–532 m borehole length, several approximately three metres long intervals occur that are composed of episyenitic rock exhibiting selective quartz dissolution. These zones are highly porous, for example as shown by the pore-water sample KFM08C-4 from 455.7 m depth along the borehole.

Fractures are abundant and occur over the entire drillcore. A total of 4,204 fractures have been mapped (i.e. approx. 5 fractures/metre) outside the crushed zones and sealed fracture network zone, with 3,525 of them being sealed, 623 being open, and 56 being partly open /Petersson et al. 2006b/. Open fractures are especially abundant in the intervals 161–191 m, 230–250 m, 419–542 m, 673–705 m, 829–832 m, and 946–949 m borehole length.

Calcite and chlorite are the most abundant minerals in open fractures often accompanied by clay minerals (illite, corrensite) and pyrite /Petersson et al. 2006b/. Less abundant are apophyllite, analcime, pyrite, laumontite, Fe-hydroxides, and asphalt, the latter being restricted to depths above 150 metres in the borehole. In closed fractures there occur in addition epidote, quartz, prehnite, adularia, unspecified sulphides, and sometimes biotite.

Table 4-1. KFM08C borehole: List of samples used for pore-water studies and experiments and measurements performed.

Sample no.	SKB sample no.	Average depth along borehole (m)	Average depth below surface (m) ¹⁾	Water loss porosity	Density	Diff. isotope equil. method	Out-diffusion experiments		
							Chemistry	⁸⁷ Sr/ ⁸⁶ Sr $\delta^{37}\text{Cl}$	Cl time-series
KFM08C-1	SKB 012108	154.69	133.97	X	X	X	X	P	X
KFM08C-2	SKB 012109	254.92	220.76	X	X	X	X	P	X
KFM08C-3	SKB 012110	353.92	306.50	X	X	X	X	P	X
KFM08C-4	SKB 012111	455.72	394.67	X	X	X	X	P	X
KFM08C-5	SKB 012112	553.20	479.08	X	X	X	X	P	X
KFM08C-6	SKB 012113	648.58	561.69	X	X	X	X	P	X
KFM08C-7	SKB 012114	751.45	650.77	X	X	X	X	P	X
KFM08C-8	SKB 012115	839.74	727.24	X	X	X	X	P	X
KFM08C-9	SKB 012116	917.21	794.33	X	X	X	X	P	X
KFM08C-10	SKB 012117	938.30	812.59	X	X	X	X	P	X

¹⁾ borehole inclination: 60°,

X = experiment performed, analytical data available,

P = experiment performed, analytical data pending.

Table 4-2. KFM08C borehole: Sample geology and distance to fractures.

Sample no.	Average borehole length (m)	Lithology	Alteration/ tectonisation ¹⁾	Fracture intensity ¹⁾
KFM08C-1	154.69	metagranite, homog. med.-grained, foliated red-grey	± 5 m	moderate
KFM08C-2	254.92	metagranite, homog. med.-grained, foliated, white-grey	± 5 m	high
KFM08C-3	353.92	metagranite, homog. med.-grained, foliated, white-grey	± 60 m	low
KFM08C-4	455.72	porous episyenite, homog. medium-grained, reddish	± 5 m	moderate
KFM08C-5	553.20	metagranite, homog. fine to med.-grained, white-grey	± 10 m	low
KFM08C-6	648.58	metagranite, homog. fine-grained, foliated, white-grey	± 10 m	low
KFM08C-7	751.45	metagranite, homog. med.-grained, foliated, white-grey	± 60 m	low
KFM08C-8	839.74	metagranite, porphyric med.-grained, foliated, grey	± 10 m	low
KFM08C-9	917.21	metagranite, porphyric med.-grained, foliated, grey	± 25 m	low
KFM08C-10	938.30	metagranite, homog. med.-grained, white-grey	± 45 m	low

¹⁾ approximate distance to next major alteration zone and fracture intensity above and below sample (from WellCAD image, /Petersson et al. 2006b/).

In spite of the intense alteration, the differential flow logging revealed only 21 flowing fractures in borehole KFM08C /Väisäsvaara et al. 2006b/. About half of these water-conducting fractures occur between 100–300 m borehole length with a low transmissivity ranging from 10^{-9} to 10^{-8} m²/s. The other half of transmissive fractures (up to $\times 10^{-7}$ m²/s) is concentrated in the strongly albitised zone between about 450 m and 530 m along borehole. The deepest water-conducting fracture was observed at 683 m depth along the borehole with a transmissivity of $6.6 \cdot 10^{-8}$ m²/s. The frequency and depth distribution of water-conducting fractures in borehole KFM08C is thus similar to borehole KFM01D (cf Figure 3-4 and /Väisäsvaara et al. 2006a/).

4.1 Water content and water-loss porosity

The water content of the metagranite samples of borehole KFM08C varies from the surface to near the end of the borehole at 938 m in the narrow range of 0.07–0.12 wt.% (Table 4-3). For all samples except for one, the gravimetric water content derived by drying (WC_{Dry}) agrees well with that determined by the diffusive isotope equilibration technique ($WC_{IsoExch}$), the latter being slightly higher as commonly observed.

A larger gravimetric water content of 3.08 wt.% is obtained for the porous episyenite sample at 455 m borehole length (Figure 4-1). This average value also includes the large-sized sample (~1 kg) used for the out-diffusion experiment. The drying time for this sample was more than 6 months until stable weight conditions were attained. In this case the $WC_{IsoExch}$ is about 10% lower than the WC_{Dry} , but still within the standard deviation of the multiple measurements of WC_{Dry} (Table 4-3). Indeed, the $WC_{IsoExch}$ of this sample appears to be more representative for the in situ water content because of the intense alteration that includes secondary clay minerals and possibly zeolites. During extended drying, zeolites could loose some crystal water leading to an overestimation of the measured WC_{Dry} . In addition, the porous texture of this rock might allow a deterioration of the gravimetrically measured water content by the influence of stress release and related induced drilling fluid contamination, but would not alter the water content determined by the diffusive isotope exchange technique. Nevertheless, the low-transmissive character of the sample has not been changed as shown by the diffusion-type curve described by the CI time-series. Moreover, the CI content calculated for the pore water using the average value for the water content fits well with the profile described by the CI content of the samples above and below (cf Section 4.3).

Within the narrow range of water contents obtained for the metagranite samples (the episyenite sample excluded) there is no significant trend developed as a function of depth, although the lowest values are recorded for samples below 750 m borehole length (Figure 4-1, Table 4-3).

The volumetrically determined bulk dry density of the metagranites is similar for all samples and varies between 2.610 g/cm³ and 2.656 g/cm³ (Table 4-4). This results in an equally similar water-loss porosity of the metagranites of 0.17–0.32 vol.%. In contrast, the bulk density of the porous episyenite is lower (2.452 g/cm³) reflecting the high degree of alteration and associated higher porosity with the water-loss porosity being 7.28 vol.% for the episyenite sample at 455 m along the borehole (Figure 4-1).

Table 4-3. KFM08C borehole: Water content derived by drying at 105°C and by the diffusive isotope equilibration method.

Laboratory sample no.	Borehole length (m)	Number of samples	Water content by drying at 105°C		Water content by diffusive isotope equilibration method	
			average (wt.%)	1 σ (wt.%)	(wt.%)	error ¹⁾ (wt.%)
KFM08C-1	154.69	3	0.079	0.003	0.099	0.006
KFM08C-2	254.92	3	0.119	0.016	0.097	0.006
KFM08C-3	353.92	3	0.103	0.015	0.088	0.003
KFM08C-4	455.72	4	3.081	0.967	2.770	0.028
KFM08C-5	553.20	3	0.065	0.017	0.100	0.004
KFM08C-6	648.58	3	0.108	0.030	0.110	0.004
KFM08C-7	751.45	3	0.069	0.015	0.093	0.005
KFM08C-8	839.74	3	0.071	0.004	0.097	0.004
KFM08C-9	917.21	3	0.098	0.002	0.146	0.005
KFM08C-10	938.30	3	0.087	0.004	0.102	0.004

¹⁾ error calculated with Gauss' law of error propagation,

²⁾ assumed error \pm 10%.

Table 4-4. KFM08C borehole: Bulk density and water-loss porosity.

Laboratory sample no.	Borehole length (m)	Number of samples	Bulk density (wet) ¹⁾ (g/cm ³)	Water-loss porosity	
				average (vol.%)	1 σ (vol.%)
KFM08C-1	154.69	3	2.651	0.21	0.01
KFM08C-2	254.92	3	2.656	0.32	0.04
KFM08C-3	353.92	3	2.631	0.27	0.04
KFM08C-4	455.72	4	2.452	7.29	2.24
KFM08C-5	553.20	3	2.634	0.17	0.05
KFM08C-6	648.58	3	2.619	0.28	0.08
KFM08C-7	751.45	3	2.645	0.18	0.04
KFM08C-8	839.74	3	2.651	0.19	0.01
KFM08C-9	917.21	3	2.641	0.26	0.01
KFM08C-10	938.30	3	2.610	0.23	0.01

¹⁾ determined from mass and volume of saturated (wet) drillcore sample used for out-diffusion experiment,

²⁾ assumed error $\pm 10\%$.

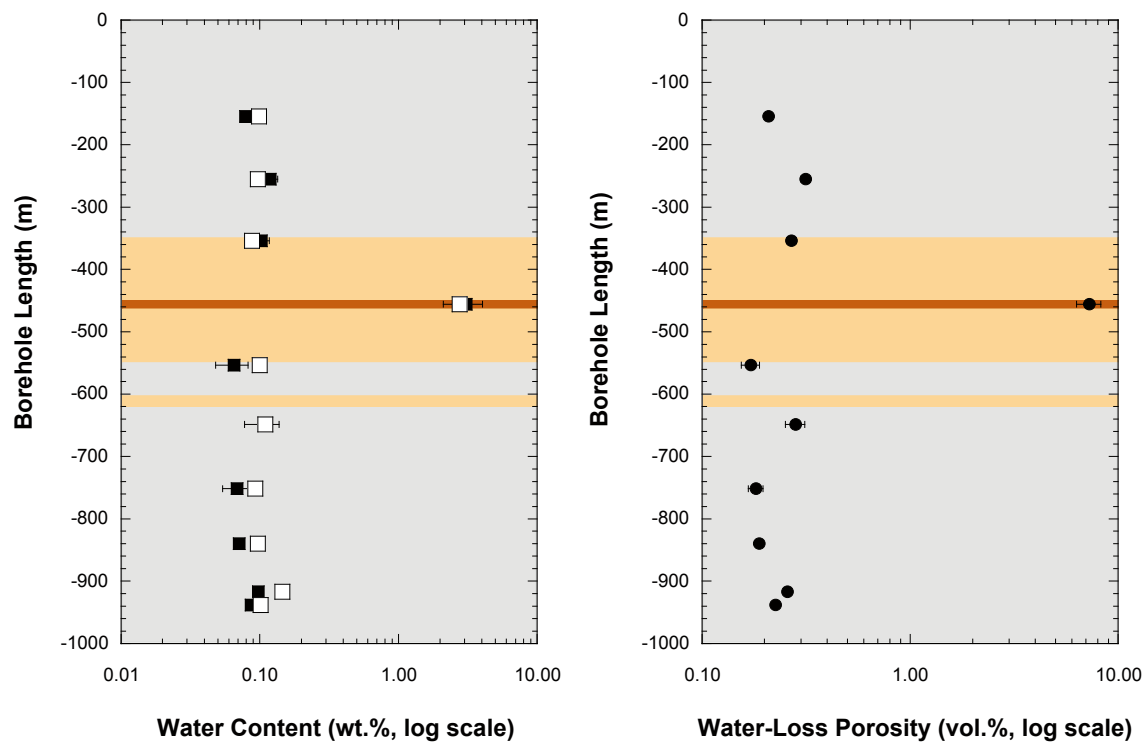


Figure 4-1. Borehole KFM08C: Water content derived by drying at 105°C to stable weight (left, closed symbols) and by the diffusive isotope equilibration method (left, open symbols), and the water-loss porosity of metagranite samples as a function of the borehole length (right). Intervals of strong albitisation are shown in tan colour, and that of the porous episyenite in brown (note the logarithmic scale of the x-axes).

4.2 Out-diffusion experiments

Out-diffusion experiments have been performed on 10 core samples from borehole KFM08C. The samples were collected on-site from fracture-free rock portions with the most proximate open and/or closed fracture being at least some 5 m away if possible. For 6 samples enough material was received to perform the out-diffusion experiment on a fracture-free core sample of 19 cm length, i.e. on a rock mass of about 1 kg. For 4 samples (KFM08C-1, -6, -7, -8) a 12 cm long core piece (approx. 0.65 kg of rock) was used for the experiments. In all experiments the weight ratio of test water to rock was kept between about 0.100 and 0.113, except for samples KFM08C-4 and 8 where it was 0.153 and 0.145, respectively (Table 4-5). The experiment temperature was 45°C for all samples.

4.2.1 Equilibrium control in out-diffusion experiment

The monitoring of steady-state conditions in the out-diffusion experiments was performed with small-sized samples of 0.5 mL that were taken at regular intervals and analysed for their anion concentration. Equilibrium conditions with respect to chloride concentrations in the remnant solution in the pore volume of the rock and the test water in the sample container is attained when the Cl time-series concentrations reach a plateau, i.e. when the concentrations remain constant. For the samples from borehole KFM08C, equilibrium conditions with respect to the chloride out-diffusion have been attained in the experiments after about 50 to 60 days and the experiment time has been fixed to 105 and 106 days, respectively to allow for complete equilibration. Figure 4-2 shows the evolution of the Cl concentration during the out-diffusion experiments of the porous episyenite sample (KFM08C-4) and the deepest metagranite sample (KFM08C-10). As can be seen from this figure, the equilibration time is similar and largely independent of the sample's porosity, its mass or sampling depth.

4.2.2 Chemical composition of experiment solutions

The chemical compositions of the supernatant solutions after termination of the out-diffusion experiments on samples from borehole KFM08C are given in Table 4-5. The pH of all solutions varies in a narrow range between 6.95 and 7.36 independent of rock type. In contrast, the total mineralisation ranges from 137 mg/L to 309 mg/L for the metagranites and is 1,289 mg/L for the episyenite (sample KFM08C-4). This higher total mineralisation is a consequence of the higher porosity of the episyenite and thus the larger amount of pore water present in the rock.

As mentioned in Section 3.2.2, the concentration of reactive compounds will have a contribution from mineral dissolution reactions that occur during the experiment. Because of the similar composition of the metagranites such contribution to the experiment solutions of these rocks can be expected to be similar. Thus, large changes in ion-ion ratios might be indicative for compositional differences in the pore water. For example, the ratio of alkaline earth elements to sodium increases with increasing depth of the metagranite samples and becomes close to unity for samples below 750 m borehole length (Figure 4-3). This is accompanied by an increase in the Cl contents of the experiment solutions from 16.5 mg/L to more than 100 mg/L at greatest depth.

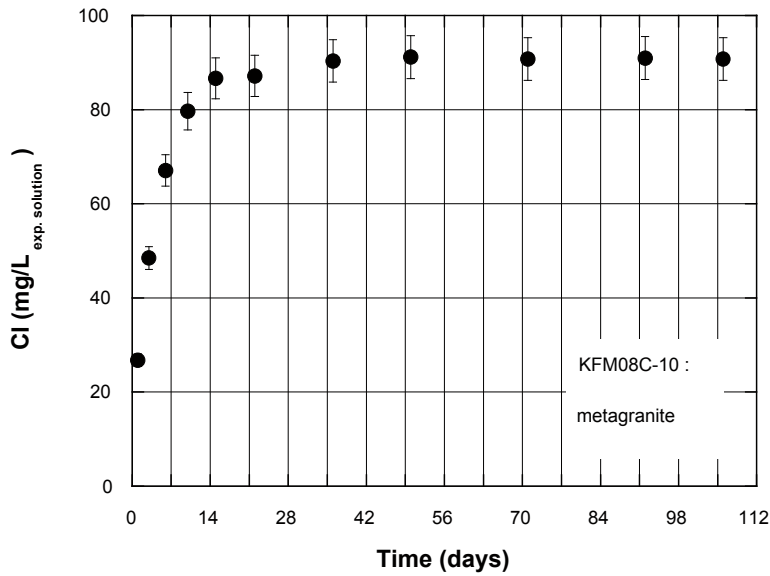
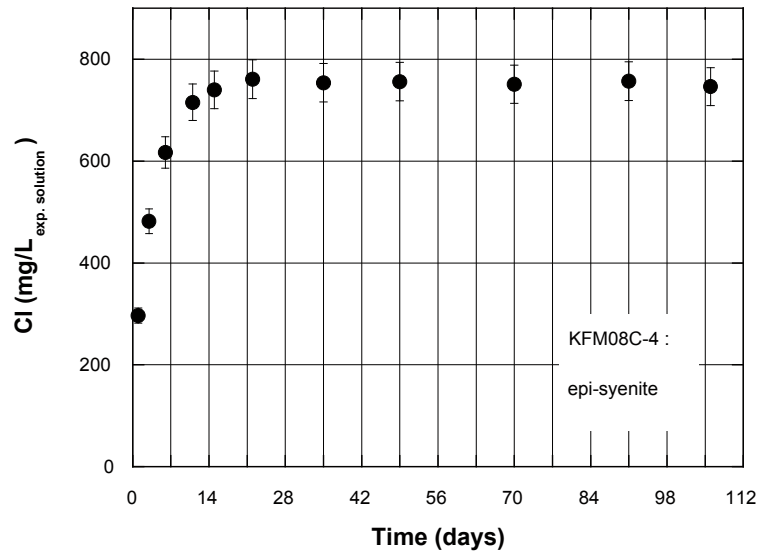


Figure 4-2. Borehole KFM08C: Chloride time-series of the highly porous episyenite sample ($\Phi_{WL} = 7.28$ vol.%, KFM08C-4, depth below surface = 394.76 m; above) and for the deepest meta-granite sample ($\Phi_{WL} = 0.23$ vol.%, KFM08C-10, depth below surface = 812.59 m; below) displaying that equilibrium conditions in the out-diffusion experiments have been achieved, but at different total concentrations.

The same general picture is obtained for the highly porous episyenite sample KFM08C-4 although at greater concentrations due to the higher pore water volume in this sample (Figure 4-3). Worth mentioning is the total alkalinity value of this sample which is the lowest of samples from borehole KFM08C. This demonstrates again that the total alkalinity measured in the experiment solutions is not directly indicative for the pore water. The chemical composition of this experiment sample solution further suggests that the pore water at this location does not represent a simple two-component mixture of known end-members such as Littorina or Baltic seawater with glacial or meteoric water. While the Cl concentration of the pore water in this sample (approx. 4.5 g/kgH₂O, see below) might suggest the presence of a Littorina seawater component, the ion-ion ratios do not support a simple mixing of such seawater with a dilute end-member. For example, this is seen from the Br·1,000/Cl ratio

(6.5 by weight), which is higher than that of Littorina seawater (approx. 3.6). Dilution with surface-derived water would lower the Br·1,000/Cl ratio of the Littorina seawater resulting in increased differences. This would also account for the ten times lower ratio of Mg/Cl in the experiment solution compared to Littorina seawater. Such difference can hardly be derived by simple mixing of Littorina seawater with dilute, surface-derived water to derive the pore water at this location, even when taking into account all possible water-rock interaction.

4.2.3 Implications for pore-water composition

The above described difference in total alkalinity between the experiment solutions of the metagranites and the porous episyenite has also implications on the chemical type of the pore water under in situ conditions. While bicarbonate (calculated from the measured total alkalinity) is a major anion and thus appears in the metagranite chemical type of all experiment solutions, it constitutes only a minor component in that of the episyenite. As will be shown below, the Cl concentration in the pore water of the episyenite is about 4.5 g/kgH₂O. It thus appears that in the pore water of samples with similar and higher Cl concentration, bicarbonate is present in low concentrations compared to the other anions such as Cl. For the borehole KFM08C samples this means that the chemistry of the pore water appears to be a Na-Ca-Cl-(HCO₃?) type from 150–350 m borehole length, a Na-Ca-Cl type between 350–650 m, and a Ca-Na-Cl type at depth > 750 m borehole length where the Cl concentrations exceed 10 g/kgH₂O (see below).

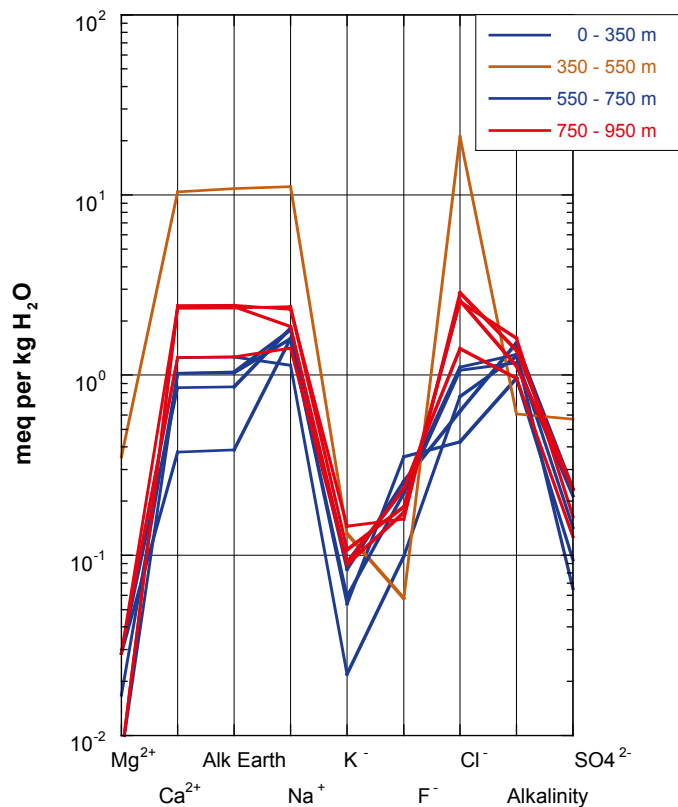


Figure 4-3. Borehole KFM08C: Schoeller diagram of experiment solutions from the drillcore samples showing the change in chemical type and degree of mineralisation as a function of the differently transmissive depth intervals. The most mineralised experiment solution is from the porous episyenite sample KFM08C-4 from the highly altered zone at 455.5 m borehole length.

Table 4-5. KFM08C borehole: Chemical composition of solutions from out-diffusion experiments at steady state conditions.

Out-diffusion experiment solution	Units	KFM08C-1	KFM08C-2	KFM08C-3	KFM08C-4	KFM08C-5	KFM08C-6	KFM08C-7	KFM08C-8
SAMPLE DESCRIPTION									
Borehole length	m	154.69	254.92	353.92	455.72	553.20	648.58	751.45	839.74
Rock type		metagranite	metagranite	metagranite	porous episyenite	metagranite	metagranite	metagranite	metagranite
Water-rock ratio		0.101	0.102	0.113	0.153	0.108	0.112	0.113	0.145
Experiment temperature	°C	45	45	45	45	45	45	45	45
Experiment time	days	105	105	106	106	106	106	106	106
MISC. PROPERTIES									
Chemical type		$\frac{\text{Na-(Ca)-}}{\text{HCO}_3\text{-Cl(F)}}$	$\frac{\text{Na-Ca-}}{\text{HCO}_3\text{-Cl}}$	$\frac{\text{Ca-Na-}}{\text{HCO}_3\text{-Cl}}$	$\frac{\text{Na-Ca-Cl}}{\text{HCO}_3\text{-Cl}}$	$\frac{\text{Na-Ca-}}{\text{HCO}_3\text{-Cl}}$	$\frac{\text{Na-Ca-}}{\text{HCO}_3\text{-Cl}}$	$\frac{\text{Ca-Na-Cl-}}{\text{HCO}_3\text{-Cl}}$	$\frac{\text{Na-Ca-Cl-}}{\text{HCO}_3\text{-Cl}}$
pH (lab)	-log(H ⁺)	6.95	7.21	7.18	6.88	7.33	7.09	7.22	7.07
Electrical conductivity	µS/cm								
Sample temperature	°C	20	20	20	20	20	20	20	20
CATIONS									
Sodium (Na ⁺)	mg/L	36.7	41.9	26.1	256.2	36.6	41.1	42.8	32.5
Potassium (K ⁺)	mg/L	2.1	3.3	0.9	5.2	2.3	3.6	3.5	3.5
Magnesium (Mg ⁺²)	mg/L	< 0.5	< 0.5	< 0.5	4.3	< 0.5	< 0.5	< 0.5	< 0.5
Calcium (Ca ⁺²)	mg/L	7.5	17.1	25.0	209.0	20.5	20.5	47.5	25.1
Strontium (Sr ⁺²)	mg/L	< 0.5	< 0.5	< 0.5	3.6	< 0.5	< 0.5	< 0.5	< 0.5
ANIONS									
Fluoride (F ⁻)	mg/L	6.7	4.9	1.9	1.1	4.2	4.4	3.3	4.5
Chloride (Cl ⁻)	mg/L	16.5	24.4	28.0	746.4	37.7	40.6	92.0	49.6
Bromide (Br ⁻)	mg/L	< 0.5	< 0.5	< 0.5	4.8	< 0.5	< 0.5	0.7	0.5
Sulphate (SO ₄ ⁻²)	mg/L	4.5	11.3	6.8	27.4	10.3	3.1	11.1	6.1
Nitrate (NO ₃ ⁻)	mg/L	4.0	< 0.5	2.9	2.7	2.0	1.6	8.6	2.5
Total alkalinity	meq/L	0.96	1.51	1.27	0.61	1.17	1.30	1.12	0.96
NEUTRAL SPECIES									
Silica (Si)	mg/L	12.10	11.90	9.39	6.45	10.60	9.10	11.00	8.63
CALC. PARAMETERS									
Total dissolved solids	mg/L	137	196	170	1,298	186	195	278	183
Charge balance	%	2.33	1.28	1.36	-0.57	-0.45	2.57	0.99	-0.12

Table 4-5. (continued)

Out-diffusion experiment solution	Units	KFM08C-9	KFM08C-10	Blank solution
SAMPLE DESCRIPTION				
Borehole length	m	917.38	938.50	
Rock type		metagranite	metagranite	
Water-rock ratio		0.105	0.101	
Experiment temperature	°C	45	45	
Experiment time	days	106	106	
MISC. PROPERTIES				
Chemical type		$\frac{\text{Ca-Na-Cl-}}{\text{HCO}_3}$	$\frac{\text{Ca-Na-Cl-}}{\text{HCO}_3}$	
pH (lab)	$-\log(\text{H}^+)$	7.28	7.36	
Electrical conductivity	$\mu\text{S/cm}$			< 10
Sample temperature	°C	20	20	20
CATIONS				
Sodium (Na^+)	mg/L	53.3	55.2	< 0.1
Potassium (K^+)	mg/L	5.7	4.2	< 0.1
Magnesium (Mg^{+2})	mg/L	< 0.1	< 0.1	< 0.5
Calcium (Ca^{+2})	mg/L	48.8	47.2	< 0.5
Strontium (Sr^{+2})	mg/L	< 0.5	< 0.5	< 0.5
ANIONS				
Fluoride (F^-)	mg/L	3.0	3.5	< 0.5
Chloride (Cl^-)	mg/L	101.5	90.8	< 0.1
Bromide (Br^-)	mg/L	1.1	1.1	< 0.5
Sulphate (SO_4^{-2})	mg/L	11.2	7.9	< 0.5
Nitrate (NO_3^-)	mg/L	1.1	1.3	< 0.5
Total alkalinity	meq/L	1.37	1.60	< 0.1
NEUTRAL SPECIES				
Silica (Si)	mg/L			< 0.01
CALC. PARAMETERS				
Total dissolved solids	mg/L	309	309	< 1.0
Charge balance	%	2.57	3.44	-

4.3 Chloride composition of pore-water

The non-destructive design of the out-diffusion experiments allows the conversion of the concentrations of chemically conservative elements in the experiment solution to in situ pore-water concentration according to equation (4). The calculated Cl concentrations in the pore water of the rock matrix of borehole KFM08C are given in Table 4-6 and graphically shown versus borehole length in Figure 4-4.

From 150–350 m along the borehole length (134–306 m below surface) Cl concentrations in the pore water vary between 2 g/kgH₂O and 3 g/kgH₂O before they gradually increase to 6 g/kgH₂O at the lower end of the intensely altered (albitised) zone (Figure 4-4). The pore-water Cl content of the porous episyenite fits well in this general increase with increasing depth. Below the zone of strong albitisation, a somewhat lower pore-water Cl content is first observed before it rises to more than 10 g/kgH₂O at depth below 750 m borehole length (650 m below surface) with a maximum value of 15 g/kgH₂O.

Borehole KFM08C displays a similar pattern in the frequency of water-conducting fractures as borehole KFM01D, although less concentrated and generally of lower transmissivity. A first accumulation of fractures in KFM08C occurs in the first 300 m along the borehole (Figure 4-4) and a second pronounced accumulation occurs between about 450 m and 540 m borehole length just below the porous episyenite in the zone of strong albitisation. In borehole KFM01D, this second accumulation occurs at shallower depth (approx. 300–440 borehole length) and is somewhat wider (cf Figure 3-4). In both boreholes the Cl concentrations in the pore water in the shallower fractured zone are similar, varying between 2 g/kgH₂O and 3 g/kgH₂O. In the deeper zone of elevated fracture frequency, however, the pore-water Cl concentrations increase in borehole KFM08C to values twice as high compared to those in borehole KFM01D. Similarly, they are about twice as high at greater depth in borehole KFM08C where there is a general absence of water-conducting fractures detectable by differential flow logging (Figure 4-4, /Väisäsvaara et al. 2006b/).

Table 4-6. KFM08C borehole: Chloride concentration of pore water.

Laboratory sample no.	Borehole length	Lithology	Pore water Cl	Pore water Cl	Pore water Cl
	(m)		(mg/kg H ₂ O)	+ error ¹⁾ (mg/kg H ₂ O)	- error ¹⁾ (mg/kg H ₂ O)
KFM08C-1	154.69	metagranite	2,117	74	69
KFM08C-2	254.92	metagranite	2,111	326	248
KFM08C-3	353.92	metagranite	3,092	507	381
KFM08C-4	455.72	porous episyenite	4,464	1,698	887
KFM08C-5	553.20	metagranite	6,241	2,212	1,291
KFM08C-6	648.58	metagranite	4,249	1,633	919
KFM08C-7	751.45	metagranite	14,686	3,971	2,572
KFM08C-8	839.74	metagranite	10,128	573	515
KFM08C-9	917.21	metagranite	11,032	278	265
KFM08C-10	938.30	metagranite	10,627	519	473

¹⁾ error based on the standard deviation of multiple water-content measurements.

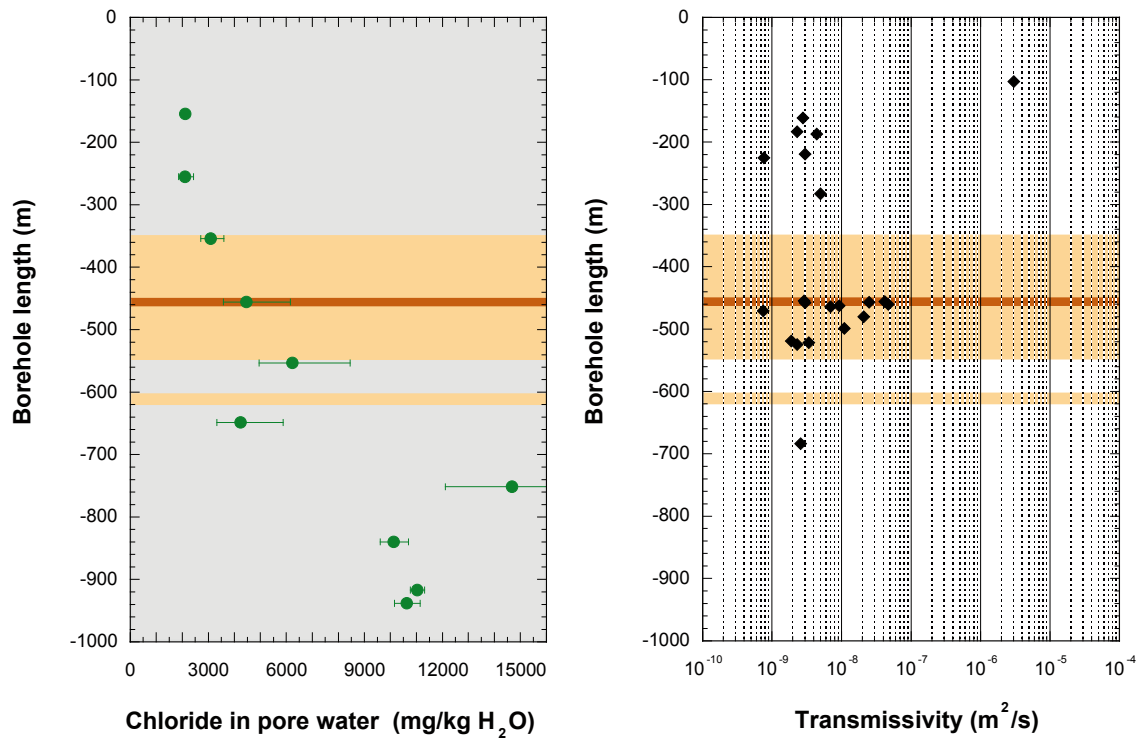


Figure 4-4. Borehole KFM08C: Chloride concentration of pore water as a function of sampling depth (left) compared to the measured hydraulic transmissivity of all detected fractures (right, data from /Väisäsvaara et al. 2006b/). Intervals of strong albitisation are shown in tan colour, and that of the porous episyenite in brown.

4.4 Water-isotope composition of pore-water

The isotopic compositions of the pore water in KFM08C highlight the strong dependency of the so-derived $\delta^{18}\text{O}$ and $\delta^2\text{H}$ values on the mass of pore water to the mass of test water used in the experiments. For most samples the error could be reduced to less than $\pm 1.5\%$ for $\delta^{18}\text{O}$ and less than $\pm 15\%$ for $\delta^2\text{H}$ by using larger volumes of rock in the experiments (Table 4-7) compared to the experiments done on material from borehole KFM01D. A low error of only $\pm 0.2\%$ and $\pm 1.6\%$ for $\delta^{18}\text{O}$ and $\delta^2\text{H}$, respectively, is obtained for the episyenite sample KFM08C-4 where the amount of pore water in the sample (average rock weight about 273 g, pore water about 6 g) is almost twice that of the test water (3.5 mL).

The isotopic composition of the pore water is shown in Figure 4-5 where it is compared with the Global Meteoric Water Line (GMWL) and proposed end-member compositions of various groundwater types /Laaksoharju et al. 1999/. The shallow pore waters have an isotopic composition that plots within a narrow range on the right of the GMWL between the “Altered Sea” reference water and the “Meteoric” reference water. They are similar in the oxygen isotope composition compared to the shallow waters of borehole KFM01D, but are less enriched in ^2H (cf Figure 3-5). Below the zone of strong albitisation the isotopic composition of the pore water (as well as the Cl concentration, see above) is close to that of the “Littorina Sea” end-member (sample KFM08C-5). Further down along the borehole and with increasing Cl concentrations the isotope composition becomes first similar to that of the “Brine” reference water (samples KFM08C-7, 8) and then more enriched in $\delta^{18}\text{O}$ at similar $\delta^2\text{H}$ values for the deepest samples (KFM08C-9, -10).

Table 4-7. KFM08C borehole: $\delta^{18}\text{O}$ and $\delta^2\text{H}$ of pore water.

Laboratory sample no.	Borehole length (m)	$\delta^{18}\text{O}^{1)}$ pore water (‰ V-SMOW)	Absolute error $\delta^{18}\text{O}^{1)}$ (‰ V-SMOW)	$\delta^2\text{H}^{1)}$ pore water (‰ V-SMOW)	Absolute error $\delta^2\text{H}^{1)}$ (‰ V-SMOW)
KFM08C-1	154.69	-8.66	3.10	-79.2	25.47
KFM08C-2	254.92	-7.44	3.06	-75.4	26.50
KFM08C-3	353.92	-7.62	1.65	-78.2	15.66
KFM08C-4	455.72	-12.69	0.15	-90.4	1.64
KFM08C-5	553.20	-5.49	2.10	-41.8	16.56
KFM08C-6	648.58	-8.31	1.51	-69.7	13.87
KFM08C-7	751.45	-8.37	2.45	-44.0	23.66
KFM08C-8	839.74	-9.59	1.52	-49.7	15.96
KFM08C-9	917.21	-3.96	1.60	-50.7	13.9
KFM08C-10	938.30	-3.59	1.95	-62.0	16.0

¹⁾ error calculated with Gauss' law of error propagation.

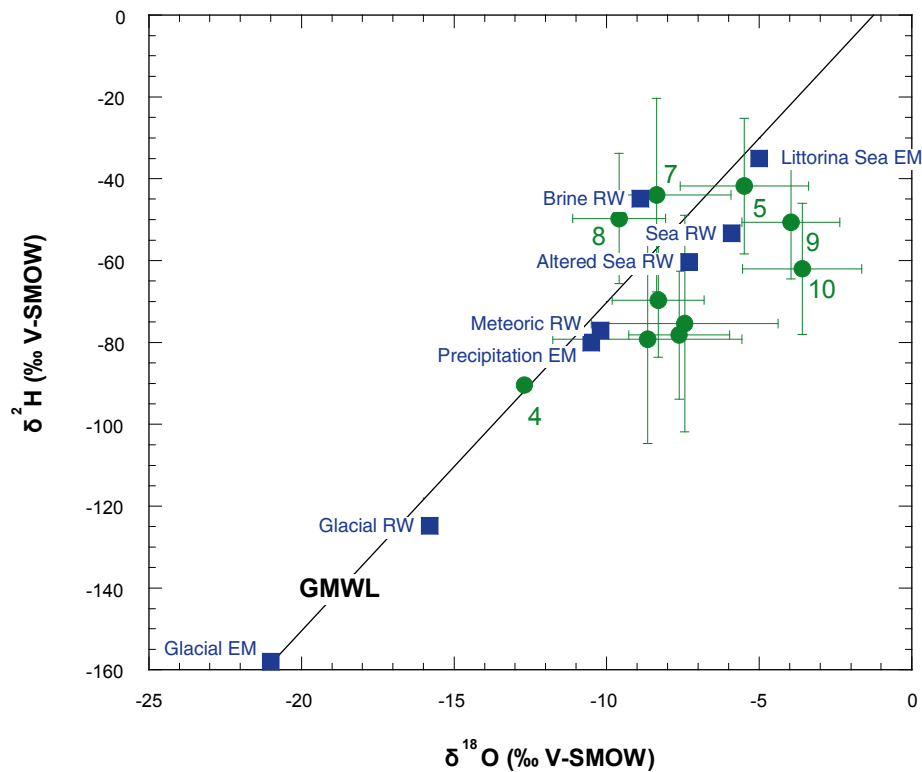


Figure 4-5. Borehole KFM08C: $\delta^{18}\text{O}$ and $\delta^2\text{H}$ values of pore water compared to the GMWL and the isotopic composition of proposed end-members (EM) and reference water (RW) compositions of various Swedish groundwaters (data from /Laaksoharju et al. 1999/). Error bars indicate cumulated error calculated with Gauss' law of error propagation and numbers indicate the sample number.

The episyenite sample KFM08C-4 at 455 m along borehole has lower $\delta^{18}\text{O}$ and $\delta^2\text{H}$ values than all other samples. They plot on the Global Meteoric Water Line below that of the “Meteoric” reference water (Figure 4-5). This suggests that the pore water contains a large component of water strongly depleted in ^{18}O and ^2H similar to that of a glacial melt water when keeping in mind the relatively high Cl concentration of 4.5 g/kgH₂O. As shown by the ion-ion ratios of Br·1,000/Cl (2.887) and Mg/Cl (0.006 by weight), the chemical composition of the experiment solution indicates, however, that this pore water is not a simple two-component mixture between a known saline end-member and a glacial melt water.

As a function of depth, the isotopic composition of pore water in borehole KFM08C is similar in the first 350 m along the borehole (Figure 4-6). At greater depth, the episyenite pore water with the very negative $\delta^{18}\text{O}$ and $\delta^2\text{H}$ values is followed by a decrease in the $\delta^{18}\text{O}$ values from 5.5‰ to 9.6‰, and the $\delta^2\text{H}$ values from -42‰ to -50‰, occur from 500 m to 850 m borehole length that is only interrupted by the $\delta^2\text{H}$ value of sample KFM08C-6, which has also a lower Cl concentration than the other samples in this interval. The two deepest samples display then the least negative $\delta^{18}\text{O}$ values (-3.6‰ and -4.0‰), while the $\delta^2\text{H}$ values remain similar to those of pore waters above.

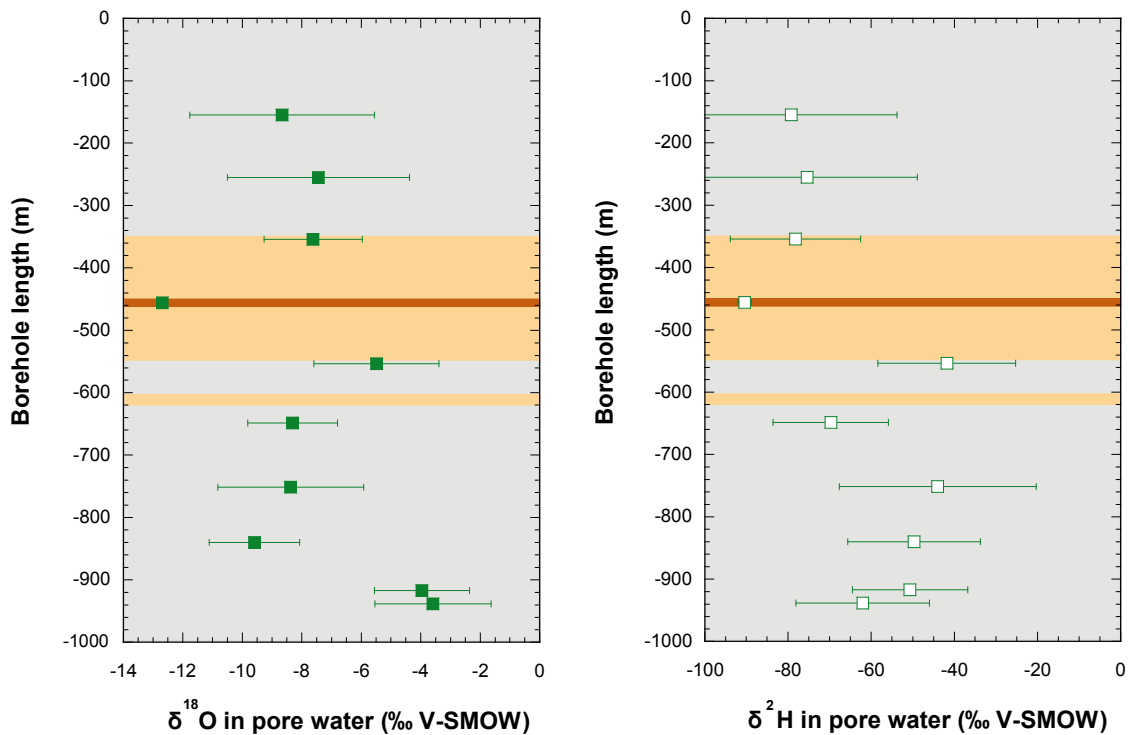


Figure 4-6. Borehole KFM08C: Depth variation of $\delta^{18}\text{O}$ and $\delta^2\text{H}$ in pore water. Error bars indicate cumulated error calculated with Gauss' law of error propagation. Intervals of strong albitisation are shown in tan colour, and that of porous episyenite in brown.

5 KFM09B borehole: Pore-water data

Borehole KFM09B was drilled at the north-western boundary of the investigation area south of the Forsmark nuclear power plant (Figure 1-1) from October 27th to December 21st, 2005. The borehole was intended to provide geological and hydrogeological information about the rock mass in a potential access tunnel area and in the central part of a potential repository. Borehole KFM09B was drilled at an inclination of 55° towards SE to a total length of 616.45 metres.

The dominant rock type encountered is a medium-grained metagranite of greyish-red to grey colour, similar to that found in other deep boreholes from the site /Petersson et al. 2006c/. About 25% of the drillcore consists of granitic pegmatite which commonly occurs in thicknesses of a few decimetres to metres. Other more subordinate rock types include amphibolite dykes, fine to medium-grained granite and fine to medium-grained metagranitoids of granodioritic composition. All rocks have experienced Svecofennian metamorphism under amphibolite conditions, except for a few veins and dykes. Rock foliation is well developed leading to a distinct anisotropy and to a gneissic appearance of certain core sections. The rocks exhibit various degrees of alteration with the most common being albitisation and oxidation evidenced in the rock as bleaching and as moderately strong haematite pigmentation, respectively.

The interval from 568.92–573.45 m borehole length comprises porous episyenitic rock that exhibits selective quartz dissolution and is similar to the episyenite at 455 m observed in borehole KFM08C (see above). The interval has a high frequency of open fractures (approx. 10 fractures per metre; /Petersson et al. 2006c/) and is expected to have an elevated transmissivity. It was decided, therefore, to take several samples for pore-water investigations along a profile away from this zone into the unaltered and unfractured host bedrock. The purpose of this sampling was to obtain information about the distance over which changes in the pore water composition in the intact bedrock can be observed. Such changes in the pore water are a result of compositional changes in the flowing water of a water-conducting zone induced by variations in palaeohydrogeological conditions.

On December 18th and 19th, 2005, a total of 8 samples were collected for pore-water characterisation in increasing intervals from decimetres to metres from the episyenite zone downwards along the borehole. The first sample, KFM09B-1, was taken at the contact of the episyenite to the metagranite. The sample is strongly altered with bleached quartz and plagioclase and reddish-coloured K-feldspar. It contains two open and two closed fissures with a green infill, all of them steeply cutting the drillcore along the borehole axis. All other samples consist of medium-grained, equigranular metagranite that are free of any fractures, but display a distinct foliation. The metagranite is mainly grey in colour with reddish-coloured K-feldspar due to pigmentation with haematite.

Unfortunately, a failure of the temperature control in the cabinet used for the diffusive isotope equilibration experiments resulted in condensation of test and pore water on the walls of the vapour-tight glass containers on 10 out of the 16 containers. The analysed isotope values of these samples show a clear deterioration induced by this condensation that can no longer be corrected for within a reasonable accuracy. Therefore, only three water contents and pore water isotope compositions derived by this method are available for borehole KFM09B.

Table 5-1 gives the list of samples used for pore-water characterisation including their SKB number, the sample numbering used in this report, and the experiments and analyses performed on each sample. The general rock type, the distance of the sample to the next proximate tectonised zone, and the frequency of open fractures /from Petersson et al. 2006c/ in the near-vicinity of each sample, are given in Table 5-2.

Table 5-1. KFM09B borehole: List of samples used for pore-water studies and experiments and measurements performed.

Sample no.	SKB sample no.	Average depth along borehole (m)	Average vertical depth below surface (m) ¹⁾	Water loss porosity	Density	Diff. isotope equil. method	Out-diffusion experiments		
							Chemistry	⁸⁷ Sr/ ⁸⁶ Sr ³⁷ Cl	Cl time-series
KFM09B-1	SKB 012100	573.47	469.76	X	X	X	X	P	X
KFM09B-2	SKB 012101	574.55	470.64	X	X	X	X	P	X
KFM09B-3	SKB 012102	576.41	472.17	X	X	X	X	P	X
KFM09B-4	SKB 012103	576.73	472.43	X	X	X	X	P	X
KFM09B-5	SKB 012104	576.98	472.63	X	X	X	X	P	X
KFM09B-6	SKB 012105	577.89	473.38	X	X	X	X	P	X
KFM09B-7	SKB 012106	582.69	477.31	X	X	X	X	P	X
KFM09B-8	SKB 012107	586.57	480.49	X	X	X	X	P	X

¹⁾ borehole inclination: 55°,

X = experiment performed, analytical data available,

P = experiment performed, analytical data pending.

Table 5-2. KFM09B borehole: Sample geology and distance to fractures.

Sample no.	Average borehole length (m)	Lithology	Alteration/ tectonisation ¹⁾	Fracture intensity ¹⁾
KFM09B-1	573.47	metagranite, heterog. med.-grained, foliated reddish	± 5 m	moderate
KFM09B-2	574.55	metagranite, homog. med.-grained, foliated, reddish-grey	± 6 m	low
KFM09B-3	576.41	metagranite, homog. med.-grained, foliated, reddish-grey	± 8 m	low
KFM09B-4	576.73	metagranite, homog. med.-grained, foliated, reddish-grey	± 8 m	low
KFM09B-5	576.98	metagranite, homog. med.-grained, foliated, reddish-grey	± 9 m	low
KFM09B-6	577.89	metagranite, homog. med.-grained, foliated, reddish-grey	± 9 m	low
KFM09B-7	582.69	metagranite, homog. med.-grained, foliated, reddish-grey	± 14 m	low
KFM09B-8	586.57	metagranite, homog. med.-grained, foliated, white-grey	± 19 m	low

¹⁾ approximate distance to major alteration zone (episyenite) and fracture intensity above and below sample (from WellCAD image, /Petersson et al. 2006c/.

5.1 Water content and porosity

The water content of the unaltered metagranite samples varies between 0.102 wt.% and 0.147 wt.% (Table 5-3). The gravimetric water content derived by drying (WC_{Dry}) agrees fairly well with that determined by the diffusive isotope equilibration technique ($WC_{IsoExch}$) for those two samples where the latter is available.

The altered sample KFM09B-1 from the contact to the episyenite has the highest gravimetric water content of 0.612 wt.% (Table 5-3). The large-sized core (approx. 0.65 kg) of this sample used for the out-diffusion experiment showed a change in weight of 0.04 g before and after the experiment, i.e. after 3 months of complete immersion in the test water. This indicates that the sample was saturated at the time of its arrival in the laboratory. For this sample $WC_{IsoExch}$, which was performed on non-fractured parts of the core, is about 15% lower than WC_{Dry} , but still within the standard deviation of the multiple measurements of WC_{Dry} (Table 5-3).

With the available data a certain contamination by drilling fluid of the sub-samples used for the gravimetric water content measurements and the out-diffusion experiment cannot be completely ruled out. Based on this probability it appears that for this sample the $WC_{IsoExch}$ is more representative for in situ conditions than WC_{Dry} .

As shown in Figure 5-1, the water contents of the metagranite samples in the unaltered rock matrix show only a small variation compared to the first metre from the episyenite contact. In this part of the rock matrix the variation is more associated to the textural heterogeneity of the rock. The same picture arises for the water-loss porosity due to the similar density values of the unaltered rocks, while the altered sample KFM09B-1 has a four to eight times higher water-loss porosity (Figure 5-1, Table 5-4).

Table 5-3. KFM09B borehole: Water content derived by drying at 105°C and by the diffusive isotope equilibration method.

Laboratory sample no.	Borehole length (m)	Number of samples	Water content by drying at 105°C		Water content by diffusive isotope equilibration method	
			average (vol.%)	1 σ (vol.%)	(wt.%)	error ¹⁾ (wt.%)
KFM09B-1	573.47	3	0.612	0.120	0.525	0.010
KFM09B-2	574.55	3	0.103	0.015	— ³⁾	— ³⁾
KFM09B-3	576.41	3	0.142	0.022	— ³⁾	— ³⁾
KFM09B-4	576.73	3	0.147	0.017	0.119	0.007
KFM09B-5	576.98	1 ²⁾	0.134	0.013	— ³⁾	— ³⁾
KFM09B-6	577.89	3	0.118	0.014	— ³⁾	— ³⁾
KFM09B-7	582.69	3	0.114	0.003	— ³⁾	— ³⁾
KFM09B-8	586.57	3	0.102	0.017	0.105	0.008

¹⁾ error calculated with Gauss' law of error propagation,

²⁾ assumed error $\pm 10\%$,

³⁾ incorrect results due to condensation/evaporation of test water during experiment.

Table 5-4. KFM09B borehole: Bulk density and water-loss porosity.

Laboratory sample no.	Borehole length (m)	Number of samples	Bulk density (wet) ¹⁾ (g/cm ³)	Water-loss porosity	
				average (vol.%)	1 σ (vol.%)
KFM09B-1	573.47	4	2.561	1.61	0.26
KFM09B-2	574.55	3	2.653	0.28	0.04
KFM09B-3	576.41	3	2.631	0.38	0.06
KFM09B-4	576.73	3	2.644	0.40	0.05
KFM09B-5	576.98	1 ²⁾	2.652	0.36	0.04
KFM09B-6	577.89	3	2.629	0.32	0.05
KFM09B-7	582.69	3	2.628	0.31	0.01
KFM09B-8	586.57	3	2.633	0.28	0.05

¹⁾ determined from mass and volume of saturated (wet) drillcore sample used for out-diffusion experiment,

²⁾ assumed error $\pm 10\%$.

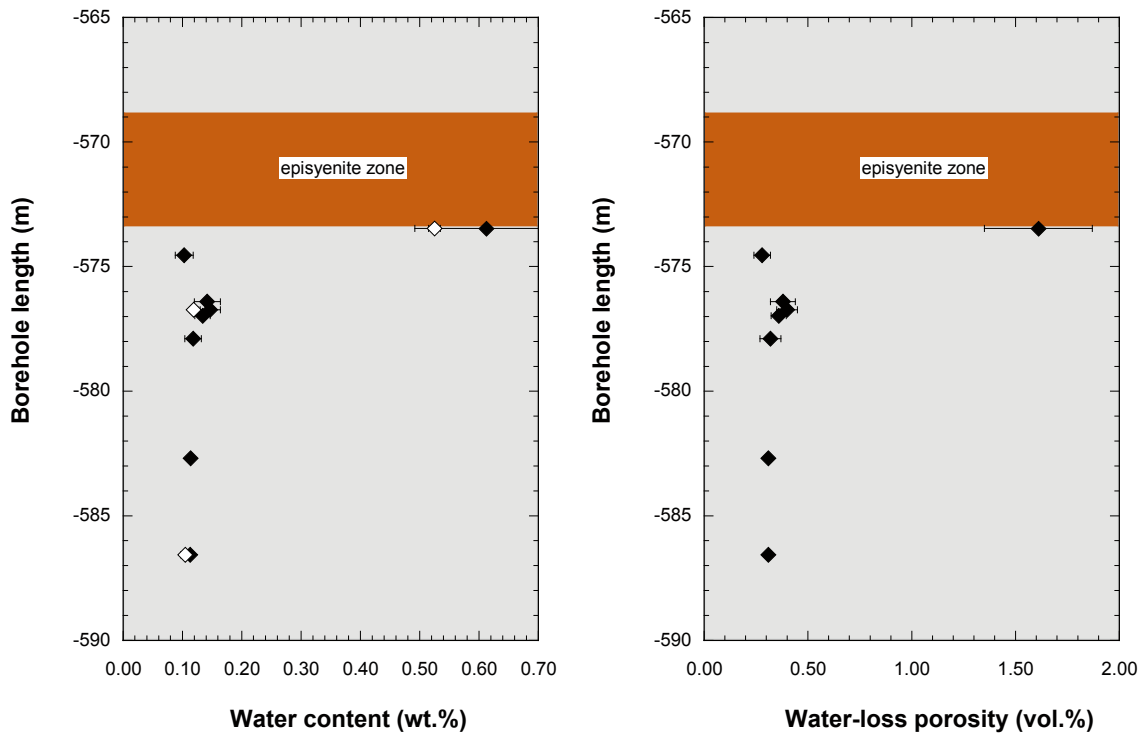


Figure 5-1. Borehole KFM09B: Water content derived by drying at 105°C to stable weight (left, closed symbols) and by the diffusive isotope equilibration method (left, open symbols), and the water-loss porosity (right) of metagranite samples along a profile away from the highly altered, porous episyenite.

5.2 Out-diffusion experiments

Out-diffusion experiments have been performed on 8 core samples from borehole KFM09B. For 6 samples enough material was received to perform the out-diffusion experiments on a fracture-free core sample of 19 cm length, i.e. on a rock mass of about 1 kg. For 2 samples (KFM09B-1 and KFM09B-5) a 12 cm long core piece (approx. 0.65 kg of rock) was used for the experiments. The weight ratio of test water to rock was between about 0.103–0.116 and the experiment temperature was 45°C for all samples (Table 5-5).

5.2.1 Equilibrium control in out-diffusion experiment

The monitoring of steady-state conditions in the out-diffusion experiments was performed with small-sized samples of 0.5 mL that were taken at regular intervals and analysed for their anion concentration. Equilibrium conditions with respect to chloride concentrations in the residual solution in the pore volume of the rock and the test water in the sample container have been attained in all experiments after about 50 to 60 days, and the experiment time has been fixed to 110 days to allow for complete equilibration.

Differences in the rock texture between the fractured sample KFM09B from the contact to the episyenite and the non-fractured samples further inside the intact rock matrix are well reflected in the evolution of the Cl concentration during the out-diffusion experiments (Figure 5-2). In the fractured sample a fairly rapid and an almost linear increase in Cl concentrations is observed between day 2 and 21 of the experiment suggesting advective mixing of pore water and test water. In the non-fractured rock samples the same time period is characterised by a slower, diffusion dominated curved increase in Cl concentration. Nevertheless, the equilibration time is similar and largely independent of the sample's porosity, its mass or texture.

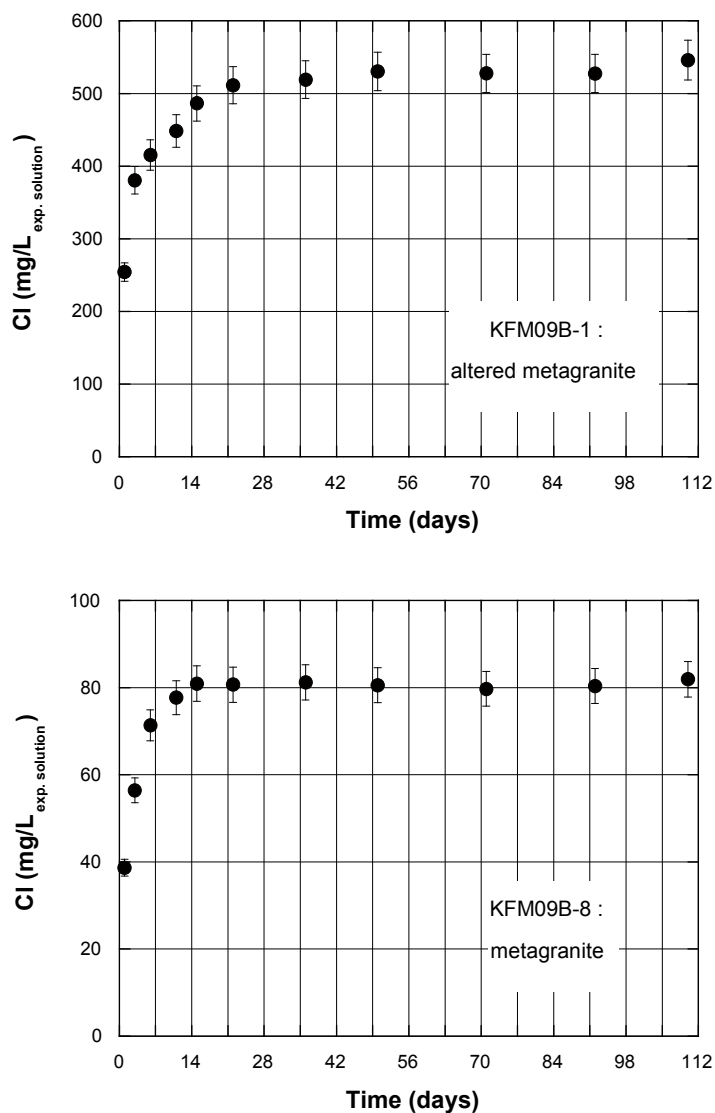


Figure 5-2. Borehole KFM09B: Chloride time-series of the altered and fractured sample KFM09B-1 (above) and the unfractured sample KFM09B-8 (below) in the intact rock matrix. The different textural state of the samples is reflected in the different slope given by the Cl concentrations in the initial phase of the experiment, but equilibrium conditions have been achieved for both samples after about 50 days.

5.2.2 Chemical composition of experiment solutions

The chemical composition of the supernatant solutions after termination of the out-diffusion experiments on samples are given in Table 5-5. The pH of all experiment solutions is around neutral as already observed for the samples from the other boreholes. The total mineralisation is similarly low for the samples from the intact matrix (215–298 mg/L), but about four times higher for the fractured sample KFM09B-1 from the contact to the episyenite. This higher total mineralisation is a consequence of the higher porosity in this sample and thus the larger amount of pore water present in the rock.

The experiment solutions of the samples from the intact rock matrix have almost equal Na concentrations while the Ca concentrations increase almost constantly with increasing distance from the episyenite. Because the contribution from mineral dissolution during the experiment will be similar, this change in the ratio of alkaline earth elements to sodium as a function of distance from the episyenite (Figure 5-3) seems to be also indicative for the pore water. In agreement with the samples from borehole KFM08C, this change is accompanied by an increase in the Cl concentrations in the experiment solution (Figure 5-3).

The experiment solution of the fractured sample KFM09B-1 from the contact to the episyenite has at higher concentrations a low ratio of alkaline earth elements to sodium and Na is the dominant cation in this solution. Similar to the episyenite sample from borehole KFM08C, it has the lowest total alkalinity value of all samples from the profile in spite of its highest mineralisation. The solution has a Br·1,000/Cl ratio (7.8 by weight) and Mg/Cl ratio (0.002 by weight) that are more similar to that of the episyenite sample from borehole KFM08C than to that of Littorina seawater. As will be shown below, the pore-water Cl concentration of this sample is also higher than that of Littorina seawater.

5.2.3 Implications for pore-water composition

As outlined above for the experiment solution of borehole KFM08C and supported here again by the solution of the porous sample KFM09B1, bicarbonate (calculated from the measured total alkalinity) is a major anion in the experiments, but will probably be at low concentrations in the pore water of these samples. Thus, the pore water of the two samples nearest to the contact to the episyenite is expected to be of a Na-Ca-Cl type. Further into the surrounding host rock, i.e. 3 metres from the contact, the pore water is of a Ca-Na-Cl chemical type although at different Cl concentrations as is shown below.

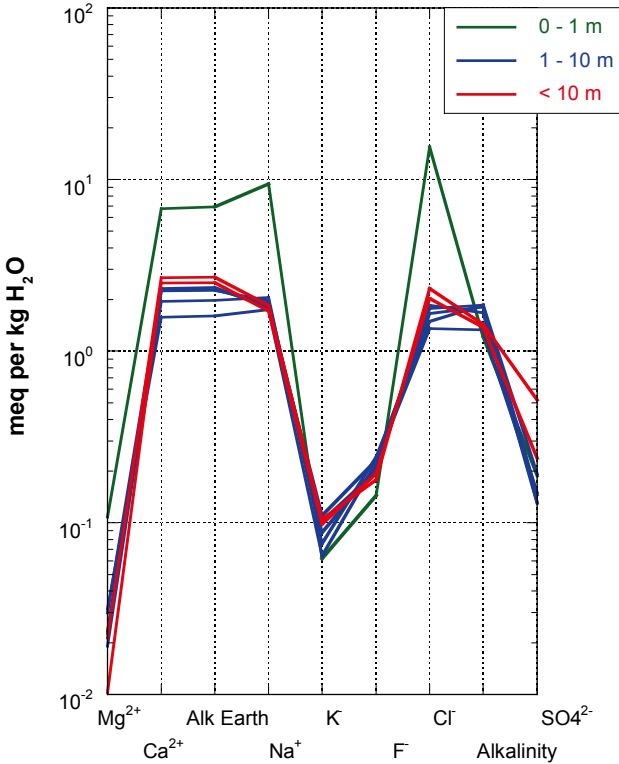


Figure 5-3. Borehole KFM09B: Schoeller diagram of experiment solutions from the drillcore samples showing the change in chemical type and degree of mineralisation along a profile away from a highly altered episyenite (figure legend gives distance from episyenite).

Table 5-5. KFM09B borehole: Chemical composition of solutions from out-diffusion experiments at steady state conditions.

Out-diffusion experiment	solution	Units	KFM09B-1	KFM09B-2	KFM09B-3	KFM09B-4	KFM09B-5	KFM09B-6	KFM09B-7	KFM09B-8	Blank solution
SAMPLE DESCRIPTION											
Borehole length		m	573.47	574.55	576.41	576.73	576.98	577.89	582.69	586.57	
Rock type			alt. m-granite	metagranite	metagranite	metagranite	metagranite	metagranite	metagranite	metagranite	
Water-rock ratio			0.112	0.104	0.105	0.106	0.112	0.116	0.103	0.107	
Experiment temperature		°C	45	45	45	45	45	45	45	45	
Experiment time		days									
MISC. PROPERTIES											
Chemical type			$\underline{\text{Na-Ca-Cl}}$	$\underline{\text{Na-Ca-Cl-HCO}_3}$	$\underline{\text{Ca-Na-HCO}_3\text{-Cl}}$	$\underline{\text{Ca-Na-Cl-HCO}_3}$	$\underline{\text{Ca-Na-HCO}_3\text{-Cl}}$	$\underline{\text{Na-Ca-HCO}_3\text{-Cl}}$	$\underline{\text{Ca-Na-Cl-HCO}_3}$	$\underline{\text{Ca-Na-Cl-HCO}_3}$	
pH (lab)		$-\log(\text{H}^+)$	6.97	7.04	7.1	7.14	7.09	7.22	6.81	6.95	
Electrical conductivity		$\mu\text{S/cm}$									< 10
Sample temperature		°C	20	20	20	20	20	20	20	20	20
CATIONS											
Sodium (Na ⁺)		mg/L	217.3	40.2	43.5	45.1	41.2	47.3	39.6	42.6	< 0.1
Potassium (K ⁺)		mg/L	2.4	2.5	4.0	3.4	4.3	3.0	3.8	4.1	< 0.1
Magnesium (Mg ⁺²)		mg/L	1.3	< 0.5	< 0.5	< 0.5	< 0.5	< 0.5	< 0.5	< 0.5	< 0.5
Calcium (Ca ⁺²)		mg/L	135.7	31.5	45.3	45.0	46.5	39.2	50.1	53.7	< 0.5
Strontium (Sr ⁺²)		mg/L	1.4	< 0.5	< 0.5	< 0.5	< 0.5	< 0.5	< 0.5	< 0.5	< 0.5
ANIONS											
Fluoride (F ⁻)		mg/L	2.7	4.3	3.8	4.0	4.4	4.6	3.7	3.4	< 0.5
Chloride (Cl ⁻)		mg/L	548.9	48.0	62.9	65.6	58.8	52.7	72.0	82.1	< 0.1
Bromide (Br ⁻)		mg/L	4.3	0.8	0.9	0.9	0.9	0.8	0.8	1.0	< 0.5
Sulphate (SO ₄ ⁻²)		mg/L	9.0	7.2	9.2	6.3	7.0	6.3	11.4	25.0	< 0.5
Nitrate (NO ₃ ⁻)		mg/L	7.4	7.8	1.9	4.1	< 0.5	4.4	6.0	2.7	< 0.5
Total alkalinity as HCO ₃ ⁻		mg/L	1.21	1.33	1.86	1.68	1.81	1.86	1.38	1.43	< 0.1
NEUTRAL SPECIES											
Silica (Si)		mg/L	9.57	11.50	9.95	10.20	11.20	8.81	9.84	11.20	< 0.01
CALC. PARAMETERS											
Total dissolved solids		mg/L	991	215	282	272	273	267	265	298	< 1.0
Charge balance		%	-2.30	3.36	2.51	4.51	4.90	3.92	4.62	1.75	-

5.3 Chloride composition of pore-water

Chloride concentrations in the pore water of the metagranite samples from borehole KFM09B are calculated according to equation (4) and given in Table 5-6. In Figure 5-4 these concentrations are graphically shown as a function of the distance to the highly fractured episyenite. The vertical depth below surface of the samples shown in this figure is 469.7 m to 480.9 m.

The pore water of the altered and fractured metagranite sample just at the contact to the episyenite at 573.5 m borehole length has a Cl concentration of about 10.5 g/kgH₂O if based on the average gravimetric water content or 12.2 g/kgH₂O if calculated using the water content derived by the diffusive isotope equilibration technique. Within only one metre from the episyenite into the intact metagranite rock matrix the pore water has dropped to a Cl concentration of 4.8 g/kgH₂O. This is maintained over the next two metres before it increases gradually to 8.6 g/kgH₂O at a distance of 13 metres from the contact (Figure 5-4).

No groundwater data sampled from a packed-off interval across the fractured episyenite zone are yet available. A “tube-sample” taken from the interval between 560 m and 585 m along borehole revealed a Cl content of 8.3 g/L. Taking the 27% contamination by drilling fluid into account the water in this section has a Cl concentration of about 11 g/L. Similar Cl concentrations of 12–13 g/L have also been found in fractured zones at similar depths from the neighbouring borehole KFM09A /Nilsson 2006/. Further, the fracture water appears to be of a Na-Ca-Cl chemical type, i.e. the same type as suggested for the pore water by the experiment solution of the out-diffusion experiment (see above). This suggests that in a small zone of only a few cm (the distance between fracture and first pore water sample) the pore water of the fractured metagranite is at or close to steady state with the fracture water circulating in the episyenite.

The strong decline of the pore-water Cl concentrations to less than half of that of the fracture water within a distance of only one metre indicates, however, that the system is in a transient state on the decimetre and metre scale. It further suggests that the circulation of such saline water in the episyenite did not yet occur over a very long time period. The pore-water data thus indicate that prior to this saline water a dilute to brackish water must have circulated in the episyenite for a considerable period of time. Such circulation produced the decrease in Cl concentration in the pore water from around 8.6 g/kgH₂O in the sample 13 metres from the contact to concentrations of around 4.8 g/kgH₂O in the samples between 3 and 4 metres from the contact.

Table 5-6. KFM09B borehole: Chloride concentration of pore water.

Laboratory sample no.	Borehole length (m)	Lithology	Pore water Cl (mg/kg H ₂ O)	Pore water Cl + error ¹⁾ (mg/kg H ₂ O)	Pore water Cl – error ¹⁾ (mg/kg H ₂ O)
KFM09B-1	573.47	altered metagranite	10,543	2,446	1,642
KFM09B-2	574.55	metagranite	4,886	825	615
KFM09B-3	576.41	metagranite	4,666	843	617
KFM09B-4	576.73	metagranite	4,753	595	475
KFM09B-5	576.98	metagranite	4,930	523	430
KFM09B-6	577.89	metagranite	5,199	715	560
KFM09B-7	582.69	metagranite	6,516	170	161
KFM09B-8	586.57	metagranite	8,666	1,723	1,230

¹⁾ error based on the standard deviation of multiple water-content measurements.

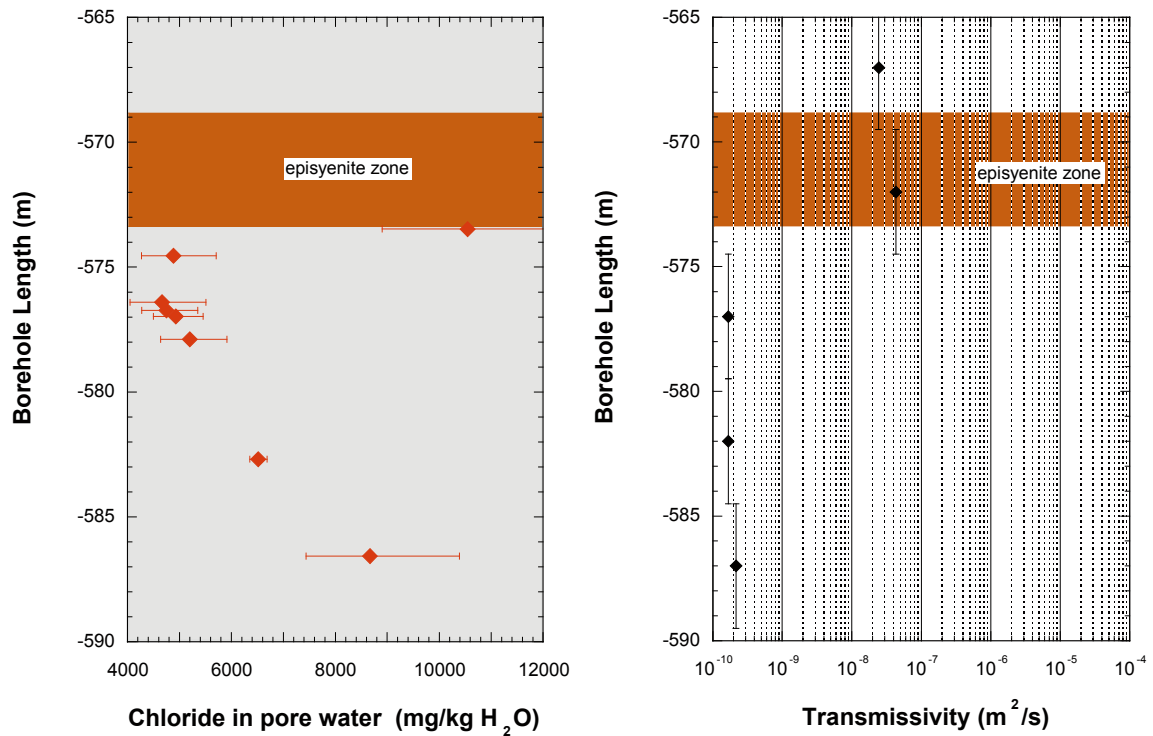


Figure 5-4. Borehole KFM09B: Chloride concentration of pore water along a profile away from a highly altered and fractured zone (left) compared to the transmissivity measured in 5 m intervals from single-hole injection tests (right, data from /Gustavsson et al. 2006/).

5.4 Water-isotope composition of pore-water

As mentioned previously, only three isotope compositions of pore water could be successfully derived due to a failure in the temperature control during the experiments. The fluctuations in temperature resulted in condensation of test and pore water on the walls of the glass containers which resulted in a fractionation of the water isotopes that can no longer be corrected for. In contrast, the three samples KFM09B-1, 4, and 8 were placed into a different cabinet and no condensation was observed in the six glass containers of these samples.

The isotopic composition of the pore water from these three samples is surprisingly similar in spite of their greatly different Cl concentrations. The $\delta^{18}\text{O}$ values vary between -4.7‰ and -6.8‰ and those of $\delta^2\text{H}$ between -46.2‰ and -52.8‰ (Table 5-7). In the $\delta^{18}\text{O}$ - $\delta^2\text{H}$ diagram the pore water isotope values plot between that of the “Altered Sea” and “Littorina” reference water slightly to the right of the Global Meteoric Water Line (Figure 5-5). Although such isotope compositions occur also in pore water of samples at comparable depths from boreholes KFM01D and KFM08C, in these latter cases they are commonly associated with Cl concentrations of less than 5 g/kgH₂O, i.e. similar to that of sample KFM09B-4. In boreholes KFM01D and KFM08C pore water samples with Cl concentrations comparable to those of samples KFM09B-1 and 8 have less negative water isotope compositions.

Table 5-7. KFM09B borehole: $\delta^{18}\text{O}$ and $\delta^2\text{H}$ of pore water.

Laboratory sample no.	Borehole length	$\delta^{18}\text{O}^{1)}$ pore water (‰ V-SMOW)	Absolute error $\delta^{18}\text{O}^{1)}$ (‰ V-SMOW)	$\delta^2\text{H}^{1)}$ pore water (‰ V-SMOW)	Absolute error $\delta^2\text{H}^{1)}$ (‰ V-SMOW)
KFM09B-1	573.47	-5.75	0.79	-46.2	6.1
KFM09B-2	574.55	- ²⁾		- ²⁾	
KFM09B-3	576.41			- ²⁾	
KFM09B-4	576.73	-4.67	2.85	-49.0	26.3
KFM09B-5	576.98	- ²⁾		- ²⁾	
KFM09B-6	577.89	- ²⁾		- ²⁾	
KFM09B-7	582.69	- ²⁾		- ²⁾	
KFM09B-8	586.57	-6.82	3.41	-52.8	21.9

¹⁾ error calculated with Gauss' law of error propagation,

²⁾ incorrect analyses due to condensation/evaporation of test water during experiment.

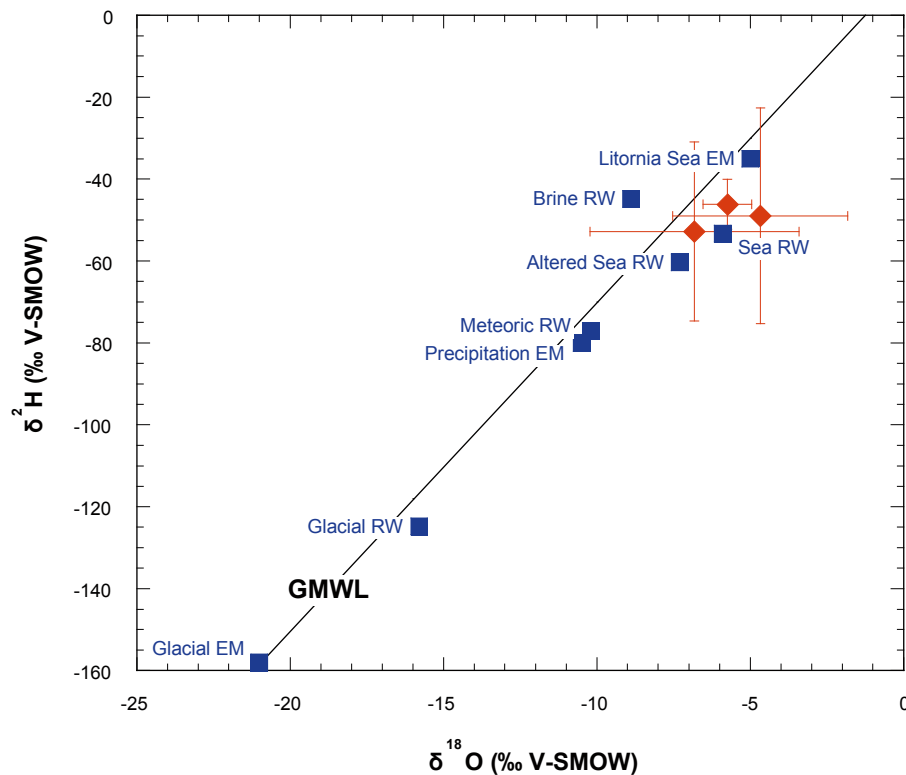


Figure 5-5. Borehole KFM09B: $\delta^{18}\text{O}$ and $\delta^2\text{H}$ values of pore water compared to the GMWL and the isotopic composition of proposed end-members (EM) and reference water (RW) compositions of various Swedish groundwaters (data from /Laaksoharju et al. 1999). Error bars indicate cumulated error calculated with Gauss' law of error propagation.

6 Discussion

The pore-water investigations performed on core samples from boreholes KFM01D, KFM08C and KFM09B clearly demonstrate that the great logistic effort to sample drillcore material in its original saturated state was well worthwhile. Water contents obtained for the rock samples by two different, largely independent methods, agree closely indicating that the core material was neither substantially influenced by de-saturation nor by drilling fluid penetration induced by immediate stress release in the borehole during and immediately following drilling. The water content and the derived water-loss porosity for borehole KFM08C show similar values in the first 500 m borehole length (~ 430 m vertical depth below surface) and then display a decreasing trend with increasing depth to 940 m borehole length (about 814 m vertical depth below surface). This is what would be expected based on the increase in lithostatic pressure and possibly also the local stress field.

The trend for the connected porosity obtained in this study contrasts, however, with that obtained from samples treated by re-saturation (Figure 6-1). For example, the porosity values reported by /Liedberg 2006/ for granitic rock samples are three to four times higher in the first 500 m along the boreholes and show an increasing trend from there to greater depth (note that the inclination of all boreholes is similar thus allowing the comparison of samples from the same structural fracture domain and similar borehole length in a first approximation). The reason for this discrepancy is explained by the re-saturation method, which delivers porosity values that are strongly affected by stress release and effects induced by sample conditioning (e.g. sawing). The smaller the size of a rock sample the larger the effect of such deterioration /e.g. Tullborg and Larson 2006/. In addition, the 7 days applied for re-saturation of the 2.5×5 cm core slices is hardly long enough for full resaturation and certainly the 6 days of subsequent drying is not long enough to remove all water from the connected pore space as shown by the much longer drying time required for the present samples to establish stable weight condition. This clearly demonstrates that the re-saturation technique applied to crystalline rocks samples from a borehole in this study is not able to produce porosity data that are reliable and representative for in situ conditions. This should also be considered in the hydrological modelling when using such data.

Boreholes KFM01D and KFM08C have been drilled into a rock domain with higher transmissivity (associated with an increase in frequency of discrete fractures) down to about 250 m borehole length and again in intervals from 350–550 m and 450–550 m, respectively (cf Figures 3-4 and 4-4). This contrasts with borehole KFM06A where a higher frequency of transmissive fractures was observed from the surface down to 450 m borehole length /Rouhiainen and Sokolnicki 2005/.

In boreholes KFM01D and KFM08C a decrease in the Cl concentration is observed again around 600–650 m borehole length (and between 700 m and 800 m in borehole KFM06A) before they increase to their highest values of 10–15 g/kgH₂O. In borehole KFM06A this decrease is again related to a higher density of water-conducting fractures and the fracture groundwater in this interval is presently much more saline than the pore water /Waber and Smellie 2007/. In boreholes KFM01D and KFM08C, however, the decreases in pore-water Cl concentration occur in a zone free of highly transmissive fractures.

A similar situation is established in borehole KFM09B at the contact of the porous and fractured episyenite zone (573 m borehole length). The Cl concentration profile developed there suggests a saline fracture groundwater with a Cl content of about 10–13 g/kgH₂O being present in the episyenite (as suggested by “tube-sample” data). The circulation of this fracture groundwater, however, did not yet occur over a very long time period as indicated by the distinct decrease in the Cl concentration of the pore water to less than 4.8 g/kgH₂O within a distance of only one metre. The adjacent smooth increase in Cl concentration to 8.6 g/kgH₂O in the sample

13 metres from the contact indicates that prior to this saline water, a dilute to brackish groundwater must have circulated in the episyenite for a considerable period of time to dilute these “initial” concentrations.

These observations suggest that dilute groundwater must have circulated over extended periods of time in at least some fracture systems down to depths of at least 500 m vertical depth below surface in boreholes KFM01D, KFM08C, and KFM09B and to about 700 m vertical depth below surface in borehole KFM06A. They also suggest that the circulation of dilute water was followed by that of saline groundwater in more recent times. The origin of this saline groundwater is not yet known because the pore water data cannot be explained by a simple combination of either of the known end-member and reference water types. Ion-ion ratios of the pore water only suggest that such saline groundwater is not of a marine origin. Similarly, the time periods of the circulation of different groundwater types (dilute and saline) are still unknown and need to be assessed by modelling. Within this context, a more constrained data set is hoped to be obtained from borehole KFM02B where a continuous profile extending from a water-conducting zone at about 500 m depth has been sampled in detail.

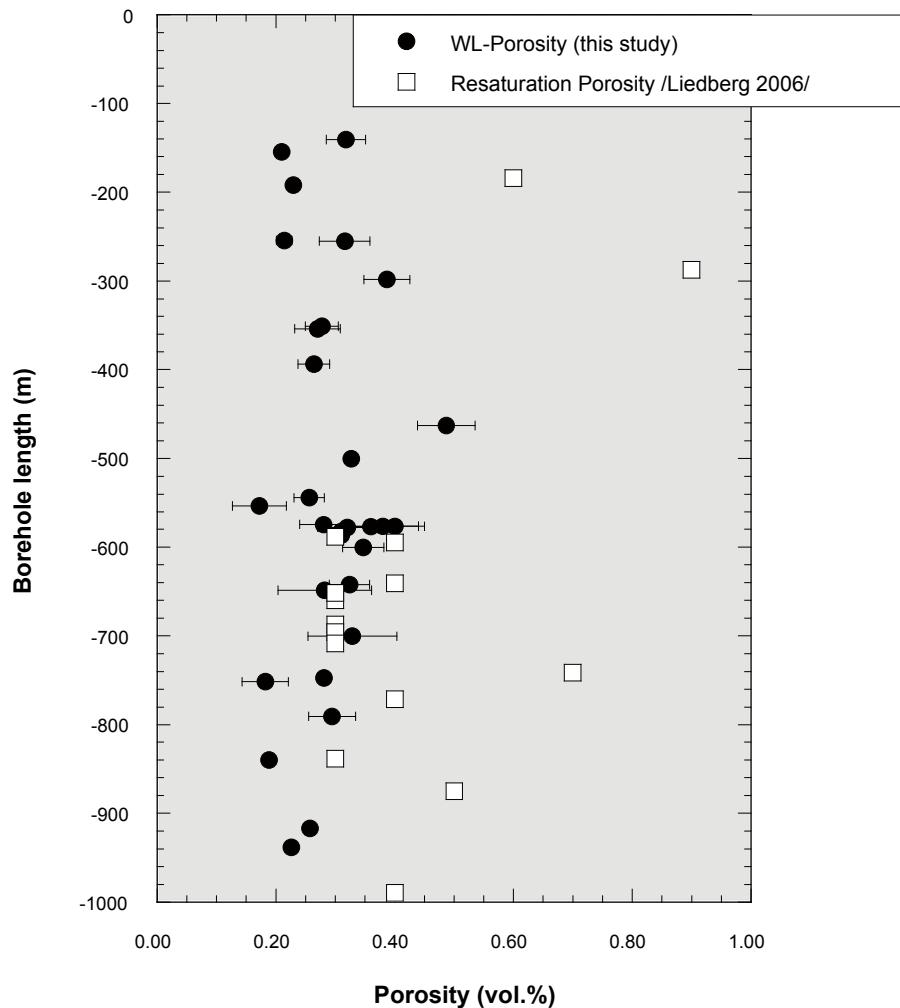


Figure 6-1. Comparison of water-loss porosity derived in this study for unaltered metagranite samples from boreholes KFM01D, KFM08C, and KFM09B, with porosity values obtained by resaturation of rock samples from boreholes KFM01A, KFM01C, KFM01D, KFM04A, and KFM05A after open surface storage (data include only granite samples from /Liedberg 2006/).

7 Acknowledgements

Much appreciation is given to Kenneth Åkerström (SKB) for the on-site selection and packaging and rapid dispatching of the drillcore samples to the University of Bern. The support and patience of Anne-Chatrin Nilsson (SKB) throughout the study was much appreciated, together with her review of this report. The considerable analytical support of R. Maeder, F. Eichinger, Ch. Läderach, and G. Chevalier (solution chemistry) at the Institute of Geological Sciences, University of Bern, is acknowledged.

References

- Carlsten S, Dose C, Gustafsson J, Petersson J, Stephens M, Thunehed H, 2006.** Forsmark site investigation. Geological single-hole interpretation of KFM09B and KFM01C. SKB P-06-135, Svensk Kärnbränslehantering AB.
- Follin S, Stigsson M, Svensson U, 2005.** Regional hydrogeological simulations for Forsmark – numerical modelling using Darcy Tools. SKB R-05-60, Svensk Kärnbränslehantering AB.
- Gustavsson E, Ludvigson J-E, Gokall-Norman K, 2006.** Forsmark site investigation: Single-hole injection tests in borehole KFM09B. SKB P-06-122, Svensk Kärnbränslehantering AB.
- Liedberg L, 2006.** Forsmark site investigation: Borehole KFM01A, KFM01C, KFM01D, KFM04A, KFM05A and KFM06A. Determination of porosity by water saturation and density by buoyancy technique. SKB P-06-234, Svensk Kärnbränslehantering AB.
- Nilsson K, 2006.** Forsmark site investigation. Hydrochemical logging in KFM09A. SKB P-06-95, Svensk Kärnbränslehantering AB.
- Petersson J, Skogsmo G, von Dalwigk I, Wängnerud A, Berglund J, 2006a.** Forsmark site investigation. Boremap mapping of telescopic drilled borehole KFM01D. SKB P-06-132, Svensk Kärnbränslehantering AB.
- Petersson J, Wängnerud A, von Dalwigk I, Berglund J, Andersson U B, 2006b.** Forsmark site investigation. Boremap mapping of telescopic drilled borehole KFM08C. SKB P-06-203, Svensk Kärnbränslehantering AB.
- Petersson J, Skogsmo G, von Dalwigk I, Wängnerud A, Berglund J, 2006c.** Forsmark site investigation. Boremap mapping of core drilled borehole KFM09B. SKB P-06-131, Svensk Kärnbränslehantering AB.
- Rouhiainen P, Sokolnicki M, 2005.** Forsmark site investigation: Difference flow logging in borehole KFM06A. SKB P-05-15, Svensk Kärnbränslehantering AB.
- Tullborg E-L, Larson S Å, 2006.** Porosity in crystalline rocks – A matter of scale. Eng. Geol., 84, 75–83.
- Tunbridge L, Panayiotis C, 2003.** Forsmark site investigation. Borehole KFM1A: Determination of P-wave velocity, transverse borehole core. SKB P-03-38, Svensk Kärnbränslehantering AB.
- Väisäsvaara J, Leppänen H, Pekkanen J, 2006a.** Forsmark site investigation: Difference flow logging in borehole KFM01D. SKB P-06-161, Svensk Kärnbränslehantering AB.
- Väisäsvaara J, Leppänen H, Pekkanen J, Pöllänen J, 2006b.** Forsmark site investigation: Difference flow logging in borehole KFM08C. SKB P-06-189, Svensk Kärnbränslehantering AB.
- Waber H N, Smellie J A T, 2005.** Forsmark site investigation. Borehole KFM06: Characterisation of pore water. Part I: Diffusion experiments. SKB P-05-196, Svensk Kärnbränslehantering AB.
- Waber H N, Smellie J A T, 2006.** Oskarshamn site investigation. Borehole KLX03: Characterisation of pore water. Part 2: Rock properties and diffusion experiments. SKB P-06-77, Svensk Kärnbränslehantering AB.
- Waber H N, Smellie J A T, 2007.** Characterisation of pore water in crystalline rocks. Appl. Geochem. (accepted).